Journal of Applied Analysis and Computation
Volume 16, Number 5, October 2026, 2668–2704
Website:http://www.jaac-online.com
DOI:10.11948/20250326

STABILITY AND BIFURCATION OF A NEUTRAL-TYPE DELAY DIFFERENTIAL GAME SYSTEM IN GREEN SUPPLY CHAINS: A GLOBAL SENSITIVITY ANALYSIS*

Hongyan Sun[1], Shuhuan Tian[1], Jianzhi Cao[2] and Pengmiao Hao[2,†]

Abstract This paper investigates a two-echelon dual-channel green supply chain via a neutral delay differential game model, focusing on supply chain coordination and system stability analysis. We compare equilibrium outcomes under centralized and decentralized decision-making, propose a transfer payment mechanism for coordination, and explore stability properties using eigenvalue methods, Sobol global sensitivity analysis, and numerical simulations. Results show that centralized decision-making outperforms decentralized decision-making in green technology level and total supply chain profit, while the transfer payment mechanism achieves Pareto improvements within a specific parameter range. Stability analysis identifies the discount rate, consumer green sensitivity, and price weight coefficient as dominant stability determinants: The price weight coefficient acts as a critical stability switch inducing Hopf bifurcation, and the discount rate extended to the real number domain directly determines equilibrium stability type. Simulations visualize stability regions and oscillation behaviors, while global sensitivity analysis quantifies parameter influences, confirming the discount rate and consumer green sensitivity as the most impactful factors. Numerical simulations further verify the theoretical findings and establish a clear link between parameter sensitivity and system stability.

Keywords Neutral delay differential game system, stability, Hopf bifurcation, dual channel green supply chain, global sensitivity analysis.

MSC(2010) 34C23.

1. Introduction

It is well known that the use of green technology can produce environmentally friendly products and reduce the damage that production activities cause to the environment. The use of green products is conducive to improving the ecological environment, developing a green industry, and promoting the sustainable development of human beings [10]. Thus, people are more willing to use green products, and then form a preference for green products [49]. Environmental awareness and preference among consumers encourage suppliers of the supply chain system to provide green

†The corresponding author.
[1]College of Data Science and Software Engineering, Baoding University, Baoding 071000, China
[2]Hebei Key Laboratory of Machine Learning and Computational Intelligence, College of Mathematics and Information Science, Hebei University, Baoding 071002, China
*The authors were supported by National Natural Science Foundation of China (12171135, 11771115) and Research Funding for High-Level Innovative Talents of Hebei University (801260201242).
Email: sunhongyan@bdu.edu.cn(H. Sun), tianshuhuan@bdu.edu.cn(S. Tian), jzcao@hbu.edu.cn(J. Cao), haopengmiao@hbu.edu.cn(P. Hao)

products [7, 15, 23, 25, 37, 41, 45, 48]. Meanwhile, manufacturers are also inspired to study green technology to improve the greenness of products [38]. Therefore, the green supply chain system (GSCS) considering green technology to reduce the resource consumption and environmental damage arises at a historic moment [8, 11, 23, 38, 43].

As is known to all, a green supply chain generally includes suppliers, manufacturers, retailers, and customers. For these companies, studying how to maximize profits is crucial. However, because of the cost of the research on green technologies, the price of green products is often much higher than that of non-green products. The price of green products will directly affect the supply and demand of products, and then influence their profits. So, setting an optimal or appropriate price for green products is vital [13, 26, 27]. Thus, finding an equilibrium between the level of green technology and the price in each of the GSCS is important.

For a GSCS, researchers tended to choose the static model or the multi-stage dynamic game model to study the game behavior between members of the discrete and intermittent supply chain [18, 42, 44]. However, the process of finding the optimal value is continuous, long-term, and dynamic, requiring real-time modeling. Differential game dynamical systems can model conflict problems and analyze variables that evolve over time. For example, Mohsin et al. proposed the green supply chain differential game system on the optimal level of green technology and the appropriate greenness [23]. Therefore, in this paper, the differential game model is used to satisfy precision and timeliness, contributing to the most suitable decisions for managers. It is noted that the manufacturer in [23] is only through the traditional retail way, that is, by a single channel. However, to accelerate the development of information and Internet technology, manufacturers have opportunities to sell directly to the customer by e-channel. Many enterprises sell not only through the traditional retail channel, but also through the electronic channel, such as Dell, Sony, Lenovo, and Hewlett Packard [6]. Both the traditional retail channel and the e-channel are used to sell green products, which is named the dual channel pattern. The dual channel supply chain system has attracted more and more attention from researchers [4, 6, 47]. For example, Zhou et al. [47] conducted a dual channel supply chain differential game system on the reduction of manufacturer emissions and retailer advertisement campaigns. Bo et al. [4] analyzed the pricing policies of a competitive dual channel GSCS. However, the dual channel green supply chain differential game system about the optimal green technology and the optimal price is still not being considered, so this work aims to construct such system.

On the other hand, in the actual supply chain system, time delay is an unavoidable phenomenon. The existence of time delay affects the stability of the system and leads to the performance changes of the whole system, such as stability switching, bifurcation, and chaos [1, 2, 9, 12, 16, 20, 21, 35, 36, 40]. Therefore, it is meaningful to consider time delay in the dual channel green supply chain differential game system. For the dual channel supply chain delay differential game model, Si et al. [31] considered product quality and analyzed the existence of Hopf bifurcation and its local asymptotic stability at equilibrium. But they consider only the situation where retailers adopt delay strategies, not the game behavior of both manufacturers and retailers adopting delay strategies, and we are interested in studying the system in which both manufacturers and retailers adopt delay strategies. So, in this paper, we focus on the optimal pricing question of dual channel green supply chain delay differential game systems in which both manufacturers and retailers adopt delay strategies and explore what dynamic behaviors occur.

During the study, the dual channel green supply chain delay differential game systems are investigated under centralized and decentralized decision making, respectively. No matter which decision making scenario is used, it aims to find the equilibrium that stands for the optimal level

of green technology and the optimal price. The optimality is proved by using the optimal control method of dynamic optimization. In this process, scholars have a tendency to construct the objective function and Hamilton-Jacobi-Bellman equation to model the final control dynamic differential system. In the past, the discount rate was used in the construction for the objective function of the infinite boundary autonomy problem and tended to be considered as a positive number, ignoring the situation of non-positive number. However, in reality, the emergence of the negative discount rate means the emergence of negative interest rates and negative economic growth. For example, throughout the 1930s and early 1940s, the nominal yields of both Treasury bonds and bills of the United States appeared to be negative as they reached maturity [5]. Redding [28] documented that the liquidity premium on these 'fugitive' bonds tends to produce surprisingly negative nominal interest rates. In September 2016, Japan, Switzerland, Sweden and Denmark had negative interest rates [3]. Furthermore, Mohsin et al. [24] claimed that COVID-19 will bring a change in the macroenvironment of the Chinese economy macro environment and will be more difficult to stabilize the economy. Its growth rate will be in the range $[-3.6\%,\ 2.8\%]$. That is, the negative interest rate and the negative growth are probably to appear. Thus, this paper extends the discount rate to the field of real numbers.

With the growing global emphasis on environmental sustainability, green supply chains (GSCs) have become a critical strategy for enterprises to balance economic performance and environmental responsibility [8, 11, 23, 38]. However, real-world GSC operations face two major challenges: Complex parameter interactions, where system behavior is governed by numerous parameters whose interactions are difficult to quantify, making it hard to identify key factors for targeted management [19, 50]; and dynamic stability risks, where time-delay effects and parameter variations can induce complex dynamic behaviors such as Hopf bifurcation, leading to system instability and performance degradation that threatens the sustainable operation of GSCs [17, 31]. Existing studies often focus on either static sensitivity analysis or isolated stability analysis, failing to establish a direct link between parameter sensitivity and system stability, This paper aims to focus on this aspect. On the one hand, it integrates Sobol global sensitivity analysis and bifurcation theory to systematically identify key parameters governing system stability, revealing that the price weight coefficient acts as a critical stability switch inducing Hopf bifurcation, and establishing a direct link between sensitivity indices and stability boundaries. On the other hand, to reflect contemporary economic conditions, based on the extension of the discount rate to the full real number domain (including negative values), it proposes a dynamic wholesale price coordination mechanism that draws on insights from sensitivity and bifurcation analysis, coordinating manufacturer and retailer behaviors while achieving Pareto improvements in supply chain profits and product greenness without compromising system stability.

The rest is organized as follows. In Section 2, the dual channel green supply chain delay differential game systems about the green technology level and the price are constructed, respectively, under centralized and decentralized decision-making situations. Moreover, the existence, the local stability for the positive equilibria, and the existence of Hopf bifurcation for the neutral delay differential system are obtained. In Section 3, by comparing two equilibria of decision-making scenarios, the decentralized the dual channel green supply chain delay differential game systems is coordinated with a contract about transfer payment mechanism so that it can make supply chain members get Pareto improvements. In Section 4, a local sensitivity analysis is carried out to study the influence of each parameter on positive equilibria. Global sensitivity analysis using the Sobol method is implemented to quantify the influence of key parameters, including the discount rate, consumer green sensitivity, and delay effects on system stability and performance. In Section 5, some numerical simulations are produced to verify and explain the

theoretical results. This paper ends with the conclusions and managerial implications.

2. Model formulation

In this section, we establish the dual channel green supply chain differential game system with delay parameter τ within a continuous time $t \in [0, +\infty)$. This system consists of the manufacturer and the retailer, and they are risk-neutral. The manufacturer and the retailer can be considered as a strategic group in a centralized decision-making situation. In this scenario, their decision-making behaviors are completely controlled by the management of green supply chain. But in decentralized decision making, they are viewed as two separate economies aiming to optimize their own profits. In addition, they form a competitive relationship. In the Stackelberg game, the leader and the follower of market competition are separately the manufacturer and the retailer.

2.1. Problem statement and assumptions

Before modeling, we introduce some notation and basic assumptions. i denotes the index of dual channel; m stands for the e-channel; r represents the traditional retail channel; $p_m^0(t)$ and $p_r^0(t)$ are separately the price of product for the retail channel and the manufacturer's e-channel; $D_m(t)$ and $D_r(t)$ are separately represent the product demand for retail channel and manufacturers' e-channel. Throughout this article, we have the following assumptions.

- The cost that the retailer sell green products is viewed as 0 [23].
- The manufacturer bears all costs of green investment and the unit cost of the product produced by the manufacturer is c_0 [23]. The use of green technology has no effect on the unit cost of green products [33].
- Both the retailer and the manufacturer adopt a delay strategy and have the same delay parameter, so the sales price of green products is

$$p_i^0(t) = \begin{cases} \theta p_i(t) + (1-\theta)p_i(t-\tau), \ t \in [0, \ +\infty), \ i = r, m, \\ \theta p_i(0) + (1-\theta)p_i(-\tau) \triangleq p_{i0}^0, \ t \in [-\tau, \ 0], \ i = r, m, \end{cases} \tag{2.1}$$

  where $p_i(t), \ i = r, m$ is the current price of channel i at time $t - \tau$; $p_m(t)$ is the current price of the online channel set by the manufacturer; $p_r(t)$ is the current price of the offline retail channel; $p_i(t-\tau)$ is on behalf of the historical price of channel i at time $t - \tau$, which serves as the state foundation for delayed pricing decisions. $p_i^0(t)$ represents the instantaneous price; The market perceived price formed by weighting the current price and historical prices. $\theta \in (0, \ 1)$ denotes the weight coefficient of the current price in the decision. Equation (2.1) reflects consumers' delayed response and price memory, where θ weights the current price and $(1-\theta)$ weights the historical price.
- Considering the case that businesses may price the products below marginal cost to attract and better target potential customers in the early stage of the formation of green products, this product itself does not make money or lose money, but as a lure to attract customers into the store. There are also two common promotion policies in our actual life: The depreciation strategy [34] and Membership card strategy [29], which can achieve 'front-end drainage, back-end realization'. Therefore, we assume that all ranges of $p_i(t), \ p_i(t-\tau)$ and $p_i^0(t)$ are $(0, \ +\infty)$ and $\tau \in [0, \ +\infty)$.

- In order to adapt to the market flexibility requirements, $D_i(t)$ $(i = r,\ m)$ is negatively related to $p_i^0(t)$ $(i = r,\ m)$ but positively correlated with the greenness function of the product $g(t)$ [23,46]. Hence, $D_i(t)$ $(i = r,\ m)$ are as follows:

$$D_m(t) = \begin{cases} \mu a - a_1 p_m^0(t) + a_2 g(t) + b p_r^0(t),\ t \in [0,\ +\infty), \\ \mu a - a_1 p_{m0}^0 + a_2 g_0 + b p_{r0}^0,\ t \in [-\tau,\ 0), \end{cases} \tag{2.2}$$

$$D_r(t) = \begin{cases} (1-\mu) a - a_1 p_r^0(t) + a_2 g(t) + b p_m^0(t),\ t \in [0,\ +\infty), \\ (1-\mu) a - a_1 p_{r0}^0 + a_2 g_0 + b p_{m0}^0,\ t \in [-\tau,\ 0), \end{cases} \tag{2.3}$$

  where a represents the total market demand; μ is representative of the initial market share of the electronic direct marketing channels; b denotes the two channel cross price elasticity coefficient; a_1 indicates the price sensitivity; a_2 means the consumer's sensitivity to the greenness of the product; $\mu \in (0,\ 1)$; $a,\ a_1,\ b,\ a_2,\ D_i(t) \in (0,\ +\infty)$.

- $g(t)$ is the greenness stock of the product at time t, which represents the cumulative environmental level and green reputation perceived by consumers. $k(t)$ is the investment level in green technology, which directly improves the product greenness. The greenness of the product differential function $g'(t)$ can be considered as

$$g'(t) = k(t) - \delta g(t),\ t \in [0,\ +\infty);\ k(t) = k_0,\ g(t) = g_0,\ t \in [-\tau,\ 0).$$

  Among them, $\delta > 0$ is the decline coefficient of the greenness of the product; The dynamic of greenness $g'(t) = k(t) - \delta g(t)$ captures the net change in environmental performance, where $\delta g(t)$ denotes the natural depreciation of green reputation. The green investment cost function $c(k(t))$ can be expressed

$$c(k(t)) = \alpha k^2(t)/2,\ t \in [0,\ +\infty),\ c(k_0) = 0,\ t \in [-\tau,\ 0),$$

  where $\alpha > 0$ expresses the green investment cost coefficient [23,33]; k_0 represents the initial level of the green technology of the product; g_0 shows the initial greenness of the product;

- Because manufacturers need to increase the investment in green technology in the process of producing green goods and the greenness of product decreases as the green technology increases over time, the coefficient of $k(t)$ is positive, but the coefficient of $g(t)$ is negative [11,23,38]. From the expression of $g'(t)$, we know that $g(t)$ and $k(t)$ are two independent functions; $g(t),\ k(t) \in (0,\ +\infty)$.

- All functions are continuous and differentiable subject to the independent variable t.

2.2. Centralized decision-making model

In the situation of centralized decision making, the purpose of modeling is to find the best sales price and the optimal level of green technology and optimize its total profit. The instantaneous total profit function is

$$\Pi^c(t) = [p_m^0(t) - c_0] D_m(t) + [p_r^0(t) - c_0] D_r(t) - c(k(t)). \tag{2.4}$$

The total instantaneous profit $\Pi^c(t)$ includes gross profits from both channels minus the cost of green investment. The firm maximizes the discounted infinite-horizon profit to determine

optimal pricing and green investment strategies. Equation (2.4) can be expanded as

$$\begin{aligned}\Pi^c(t) = {} & [p_m^0(t) - c_0][\mu a - a_1 p_m^0(t) + a_2 g(t) + b p_r^0(t)] \\ & + [p_r^0(t) - c_0][(1-\mu)a - a_1 p_r^0(t) + a_2 g(t) + b p_m^0(t)] - \alpha k^2(t)/2.\end{aligned}$$

In this decision scenario, the present value of $\Pi^c(t)$ should be maximized, so the objective function is

$$\max \int_0^{+\infty} e^{-\rho t}\ \Pi^c\ (t)dt, \tag{2.5}$$

$$\text{s.t.}\ \ \mathrm{g}'(\mathrm{t}) = \mathrm{k}(\mathrm{t}) - \delta \mathrm{g}(\mathrm{t}), \tag{2.6}$$

where $\rho \in R$ represents the discount rate and (2.6) is the state equation, which belongs to the infinite boundary autonomy problem.

The associated current-value Hamilton function of the objective function (2.5) is

$$H_c(t) = \Pi^c\ (t) + m(t)g'(t),$$

where $m(t) = e^{\rho t}\lambda(t)$ is the current value multiplier; $\lambda(t)$ is the marginal value of the state variable $g(t)$ discounted from time t to time 0; $m(t)$ is the marginal value of $g(t)$ at time t. Moreover, $\lambda(t)$ satisfies $\lim\limits_{t\to+\infty} \lambda(t) = 0$ and

$$\lambda'(t) = -e^{-\rho t}\frac{\partial H_c(t)}{\partial g(t)} = -e^{-\rho t}\frac{\partial \Pi^c(t)}{\partial g(t)} - \lambda\frac{\partial g'(t)}{\partial g(t)}.$$

Thus, the first necessary condition for maximizing $H_c(t)$ can be obtained, which is the following adjoint equation

$$m'(t) = \rho m(t) - \frac{\partial H_c(t)}{\partial g(t)} = (\rho+\delta)m(t) - a_2(p_m^0(t) + p_r^0(t) - 2c_0). \tag{2.7}$$

The optimal conditions are also available and can be separately given by

$$\frac{\partial H_c(t)}{\partial p_m^0(t)} = \mu a - 2a_1 p_m^0(t) + 2b p_r^0(t) + a_2 g(t) + (a_1 - b)c_0 = 0, \tag{2.8}$$

$$\frac{\partial H_c(t)}{\partial p_r^0(t)} = (1-\mu)a - 2a_1 p_r^0(t) + 2b p_m^0(t) + a_2 g(t) + (a_1 - b)c_0 = 0, \tag{2.9}$$

$$\frac{\partial H_c(t)}{\partial k(t)} = m(t) - \alpha k(t) = 0. \tag{2.10}$$

Deducing from the first-order equations (2.8) and (2.9), we can obtain the following cases.

- If $a_1 = b$, then the optimal greenness $g(t) = -a/2a_2 < 0$, which contradicts $g(t) > 0$;
- If $a_1 \neq b$, then the pricing strategy equations can be obtained, i.e.

$$p_m^0(t) = \frac{a_2 g(t)}{2(a_1 - b)} + \frac{[a_1\mu + b(1-\mu)]a}{2(a_1^2 - b^2)} + \frac{c_0}{2}, \tag{2.11}$$

$$p_r^0(t) = \frac{a_2 g(t)}{2(a_1 - b)} + \frac{[b\mu + a_1(1-\mu)]a}{2(a_1^2 - b^2)} + \frac{c_0}{2}. \tag{2.12}$$

In general, the price function $p_m^0(t),\ p_r^0(t)$ increases with the greenness function $g(t)$. So, in the following research, we always assume $a_1 > b$. Meanwhile,

$$p_m^0(t) - p_r^0(t) = (2\mu - 1)a/[2(a_1 + b)], \tag{2.13}$$

$$g(t) = \frac{2(a_1 - b)p_m^0(t)}{a_2} - \frac{[a_1\mu + b(1-\mu)]a}{a_2(a_1 + b)} - \frac{(a_1 - b)c_0}{a_2}. \tag{2.14}$$

Solving the derivative at time t of equations (2.11) and (2.12), and associating the common state equation (2.6) and the price function (2.1), there are

$$\theta\frac{dp_i(t)}{dt} + (1-\theta)\frac{dp_i(t-\tau)}{dt} = \frac{dp_i^0(t)}{dt} = \frac{a_2 g'(t)}{2(a_1 - b)} = \frac{a_2}{2(a_1 - b)}(k(t) - \delta g(t)),\ i = m,\ r.$$

Next, this paper also investigates the changing law of $k(t)$. Equation (2.10) takes the derivative with respect to t, deducing that

$$k(t) = m(t)/\alpha,\ k'(t) = m'(t)/\alpha. \tag{2.15}$$

Moreover, after combining and sorting equations (2.15), (2.7), and (2.13), there is

$$k'(t) = (\rho + \delta)k(t) - \frac{2a_2}{\alpha}p_r^0(t) + \frac{(1-2\mu)aa_2}{2\alpha(a_1 + b)} + \frac{2a_2c_0}{\alpha}. \tag{2.16}$$

From equation (2.16), $\partial k'(t)/\partial p_r^0(t) < 0$, which means that $k'(t)$ decreases with increasing $p_r^0(t)$. That is, as $p_r^0(t)$ is optimal, $k(t)$ and $c(k(t))$ will remain unchanged. Namely, there is $p_r^0(t) = p_{r1}^{0*}$, such that $\partial k(t)/\partial p_r^0(t) = 0$. Associating with equation (2.14), there is the dual channel green supply chain differential game system with delay about $p_m(t)$ and $p_r(t)$, which is a linear neutral delay differential system as follows

$$\begin{cases} \dfrac{dk(t)}{dt} = (\rho + \delta)k(t) - \dfrac{2a_2\theta}{\alpha}p_r(t) - \dfrac{2a_2(1-\theta)}{\alpha}p_r(t-\tau) + \dfrac{(1-2\mu)aa_2}{2\alpha(a_1 + b)} + \dfrac{2a_2c_0}{\alpha}, \\ \theta\dfrac{dp_m(t)}{dt} + (1-\theta)\dfrac{dp_m(t-\tau)}{dt} = \dfrac{a_2}{2(a_1 - b)}k(t) - \delta\theta p_m(t) - \delta(1-\theta)p_m(t-\tau) \\ \qquad\qquad + \dfrac{[a_1\mu + b(1-\mu)]\delta a}{2(a_1^2 - b^2)} + \dfrac{\delta c_0}{2}. \end{cases} \tag{2.17}$$

Remark 2.1. From the above analysis, one can model other differential systems on the basis of their focus questions. For example, the dynamic control delay system with respect to $k(t)$ and the online price $p_m(t)$; the delay differential model with respect to the green level of the product $g(t)$ and $p_m(t)$, or $g(t)$ and $p_r(t)$; the ordinary differential equations about $g(t)$ and $k(t)$, or $g(t)$ and the current value multiplier $m(t)$. In this paper, the choice of model about $k(t)$ and $p_r(t)$ is similar to system (2.17) because their equilibria are the same.

Remark 2.2. The model involves two types of variables: State variables and control variables. State variables describe the dynamic evolution of the system over time and cannot be directly controlled, such as $g(t)$, $p_r(t-\tau)$ and $p_r(t-\tau)$. Control variables are decision tools that can be directly adjusted by the firm, such as $p_m(t)$, $p_r(t)$, $k(t)$, $p_r^0(t)$ and $p_m^0(t)$.

Next, we focus on studying the existence of equilibria as the system (2.17) is equilibrated, e.g. $k'(t) = 0 = p_m'^0(t)$.

2.2.1. Existence of the non-trival equilibrium

The associated ordinary differential system of model (2.17) is

$$\begin{cases} \dfrac{dk(t)}{dt} = (\rho+\delta)k(t) - \dfrac{2a_2}{\alpha}p_r^0(t) + \dfrac{(1-2\mu)aa_2}{2\alpha(a_1+b)} + \dfrac{2a_2c_0}{\alpha}, \\ \dfrac{dp_m^0(t)}{dt} = \dfrac{a_2}{2(a_1-b)}k(t) - \delta p_m^0(t) + \dfrac{[a_1\mu+b(1-\mu)]\delta a}{2(a_1^2-b^2)} + \dfrac{\delta c_0}{2}. \end{cases} \tag{2.18}$$

We first clarify the mathematical consistency of system (2.18). Derived from the first-order optimality conditions of the centralized differential game, the state equation of product greenness $g'(t) = k(t) - \delta g(t)$, and the delayed pricing rule, system (2.18) maintains complete logical consistency with the preceding modeling framework. All variables and parameters in system (2.18) satisfy the economic assumptions: $k(t), p_m^0(t) \in (0, +\infty)$, $\rho > 0$, $\delta > 0$, $\alpha > 0$, $a_1 > b > 0$, and $a_2 > 0$. The dimensions of both sides of each equation are consistent (rate of change per unit time), and there are no contradictions in variable definitions or parameter constraints.

Next, we discuss the well-posedness of system (2.18). System (2.18) is a linear nonhomogeneous ordinary differential equation system with constant coefficients, which can be written in matrix form as

$$\dot{\mathbf{x}}(t) = \mathbf{A}\mathbf{x}(t) + \mathbf{C},$$

where $\mathbf{x}(t) = [k(t), p_m^0(t)]^\top$, $\mathbf{A}$ is the constant coefficient matrix, and $\mathbf{C}$ is the constant vector. By the fundamental theorem of linear ordinary differential equations, for any given initial condition $\mathbf{x}(0) = [k_0, p_{m0}^0]^\top$, system (2.18) admits a unique global solution. Moreover, the solution depends continuously on the initial conditions and all model parameters, which guarantees that small perturbations in initial values or parameters will not lead to drastic changes in the solution trajectory. Eigenvalue analysis further reveals that system (2.18) has a saddle-point equilibrium, which is consistent with the typical stability properties of differential game models.

Clearly, (0, 0) is not the equilibrium of system (2.18). As $k(t) = 0$, which means that, the product is the origan non-green product. The situation about non-green products is omitted because it has been studied by many scholars [6, 17, 47]. As $p_m^0(t) = 0$, namely, price products as free, which seems unlikely to happen under normal circumstances. So we focus on the case of positive equilibria.

Theorem 2.1. *Suppose that $a_1 > b$. If the parameters satisfy $A_1A_2 > 0$, and*

$$A_1 = a_2[a + 2(b-a_1)c_0],\ A_2 = 2[\alpha\delta(\rho+\delta)(a_1-b) - a_2^2],$$

then there is a unique non-trivial equilibrium $E_1(k_1^*,\ p_{m1}^{0*})$, where

$$k_1^* = \frac{\delta A_1}{A_2},\ p_{m1}^{0*} = \frac{a_2A_1}{2(a_1-b)A_2} + \frac{[a_1\mu+b(1-\mu)]a}{2(a_1+b)(a_1-b)} + \frac{c_0}{2}.$$

As the system is in equilibrium, if

$$a > \max\{[(a_1-b)c_0 - a_2g_1^*]/\mu,\ [(a_1-b)c_0 - a_2g_1^*]/(1-\mu)\},$$

then the other corresponding positive values can be obtained as follows,

$$p_{r1}^{0*} = \frac{a_2A_1}{2(a_1-b)A_2} + \frac{[b\mu+a_1(1-\mu)]a}{2(a_1+b)(a_1-b)} + \frac{c_0}{2},\ g_1^* = \frac{A_1}{A_2},\ m_1^* = \alpha k_1^*,$$
$$D_{r1}^* = \frac{a_2A_1}{2A_2} + \frac{(1-\mu)a}{2} + \frac{(b-a_1)c_0}{2},\ D_{m1}^* = \frac{a_2A_1}{2A_2} + \frac{\mu a}{2} + \frac{(b-a_1)c_0}{2}.$$

Proof. By computing the associated equation group $k'(t) = 0,\ p_m'^0(t) = 0$ of system (2.18), we can directly obtain the value of k_1^* and p_{m1}^{0*}. Recall that equilibrium E_1 also needs to satisfy the optimal conditions

$$g'(t) = k(t) - \delta g(t) = 0,\ m'(t) = \alpha k'(t) = 0.$$

Thus, $k_1^* = \delta g_1^*,\ m_1^* = \alpha k_1^*$. If these parameters satisfy $A_1A_2 > 0$, one can easily deduce that $g_1^* = \frac{A_1}{A_2} > 0$. So $k_1^*,\ m_1^* > 0$. Notice that $a_1 > b$, $\mu < 1$ and

$$p_{m1}^{0*} = \frac{a_2 g_1^*}{2(a_1 - b)} + \frac{[a_1\mu + b(1-\mu)]a}{2(a_1+b)(a_1-b)} + \frac{c_0}{2},\ p_{r1}^{0*} = \frac{a_2 g_1^*}{2(a_1 - b)} + \frac{[b\mu + a_1(1-\mu)]a}{2(a_1+b)(a_1-b)} + \frac{c_0}{2},$$

so p_{m1}^{0*} and p_{r1}^{0*} are positive as long as $A_1A_2 > 0$. Note that the definition of D_{m1}^* and D_{r1}^*, replacing p_{m1}^{0*} and p_{r1}^{0*} in equations (2.2) and (2.3), and we get

$$D_{m1}^* = \frac{\mu a}{2} + \frac{a_2 g_1^*}{2} + \frac{(b-a_1)c_0}{2},\ D_{r1}^* = \frac{(1-\mu)a}{2} + \frac{a_2 g_1^*}{2} + \frac{(b-a_1)c_0}{2}.$$

As $a > \max\{[(a_1-b)c_0 - a_2 g_1^*]/\mu,\ [(a_1-b)c_0 - a_2 g_1^*]/(1-\mu)\}$, we can also make sure that D_{m1}^* and D_{r1}^* are positive. □

Remark 2.3. As $\theta = 1$ or $\tau = 0$, $\mu = b = 0$ and $i \neq m$, equation (2.18) becomes a single channel green chain system without delay term, and the existence and stability of equilibria for this model has been obtained in [23]. So we do not study this case here.

2.2.2. Stability of the non-trivial equilibrium

Next, we study the stability of the equilibrium $E_1(k_1^*,\ p_{m1}^{0*})$ of system (2.17). Set $\tilde{k}(t) = k(t) - k_1^*,\ \tilde{p}_m(t) = p_m(t) - p_{m1}^{0*}$. For convenience, removing the sign $\sim$, system (2.17) can be rewritten as the following linear model:

$$\begin{cases} \dfrac{dk(t)}{dt} = (\rho+\delta)k(t) - \dfrac{2a_2\theta}{\alpha}p_r(t) - \dfrac{2a_2(1-\theta)}{\alpha}p_r(t-\tau), \\ \theta\dfrac{dp_m(t)}{dt} + (1-\theta)\dfrac{dp_m(t-\tau)}{dt} = \dfrac{a_2}{2(a_1-b)}k(t) - \theta\delta p_m(t) - (1-\theta)\delta p_m(t-\tau). \end{cases} \tag{2.19}$$

After translation transformation, the equilibrium E_1 of system (2.17) transforms $(0,\ 0)$ of model (2.19). Assume that $k(t) = e^{\gamma t}\varphi,\ p_m(t) = e^{\gamma t}\psi$ denote the general solution of model (2.19). γ and (φ, ψ) are separately the eigenvalue and eigenvector of its characteristic equation. Substituting them into (2.19), we can obtain the matrix form of the characteristic equation about γ, which is

$$\begin{bmatrix} \gamma - (\rho+\delta) & \dfrac{2a_2\theta}{\alpha} + \dfrac{2a_2(1-\theta)}{\alpha}e^{-\gamma\tau} \\ -\dfrac{a_2}{2(a_1-b)}\theta\gamma + (1-\theta)\gamma e^{-\gamma\tau} + \delta\theta + \delta(1-\theta)e^{-\gamma\tau} & \end{bmatrix} \begin{bmatrix} \varphi \\ \psi \end{bmatrix} = 0.$$

So, the characteristic equation of (2.19) is

$$[\theta\gamma + (1-\theta)\gamma e^{-\gamma\tau} + \delta\theta + \delta(1-\theta)e^{-\gamma\tau}][\gamma - (\rho+\delta)] + \frac{a_2}{2(a_1-b)}[\frac{2a_2\theta}{\alpha} + \frac{2a_2(1-\theta)}{\alpha}e^{-\gamma\tau}] = 0. \tag{2.20}$$

Equation (2.20) becomes a second-degree exponential polynomial equation

$$(\gamma^2 - \rho\gamma + S_1)\theta + (1-\theta)(\gamma^2 - \rho\gamma + S_1)e^{-\gamma\tau} = 0, \tag{2.21}$$

where

$$S_1 \triangleq [a_2^2 - \delta\alpha(a_1 - b)(\rho + \delta)]/[\alpha(a_1 - b)] = -A_2/[2\alpha(a_1 - b)].$$

As $\theta = 1$ or $\tau = 0$, the corresponding characteristic equation is

$$\gamma^2 - \rho\gamma + S_1 = 0. \tag{2.22}$$

From the expression of S_1, we know that $S_1 < 0 (> 0)$ if $A_2 > 0 (< 0)$. By [39] and the Vieta theorem, we can directly obtain the following lemma.

Lemma 2.1. *For equation (2.22), the following results hold:*

(I) *As $A_2 > 0$, then equation (2.22) has a positive root and a negative root.*

(II) *As $A_2 < 0$, if $\rho > 0$, then all roots of equation (2.22) have positive real parts; if $\rho < 0$, then all roots of equation (2.22) have negative real parts; if $\rho = 0$, then equation (2.22) has a pair of purely imaginary roots $\pm i\sqrt{S_1}$.*

Note that $\rho^2 - 4S_1 = [2A_2 + \rho^2\alpha(a_1 - b)]/[\alpha(a_1 - b)]$ and $a_1 > b$, so we have the following result.

Theorem 2.2. *Suppose that $a_1 > b$, $A_1A_2 > 0$ are satisfied, if the parameters satisfy*

(i) *$A_2 > 0$, then the unique positive equilibrium E_1 is a saddle;*

(ii) *$A_2 < 0$, $\rho > 0$ and $2A_2 + \rho^2\alpha(a_1 - b) > 0$ (< 0), then E_1 is an unstable node (focus);*

(iii) *$A_2 < 0$, $\rho < 0$ and $2A_2 + \rho^2\alpha(a_1 - b) > 0$ (< 0), then E_1 is an asymptotically stable node (focus);*

(iv) *$A_2 < 0$, $\rho = 0$, then E_1 is the center of system (2.18).*

Remark 2.4. From $A_1A_2 > 0$, one can deduce that $A_2 \neq 0$ and $S_1 \neq 0$. Thus $\gamma = 0$ is not the eigenvalue of equation (2.22). So system (2.18) does not undergo a transcritical bifurcation near E_1.

Remark 2.5. In the Subsection 2.1, we consider the special case that businesses may price the products below marginal cost to attract customers in the early stage of the formation of green products, so all the ranges of $p_i(t)$, $p_i(t - \tau)$ and $p_i^0(t)$ are $(0, +\infty)$. If this special case is not considered, then $p_i(t)$, $p_i(t - \tau)$ and $p_i^0(t)$ are $(c_0, +\infty)$. Now, one can deduce that $a > 2(a_1 - b)c_0$, so $A_1 > 0$ is always satisfied and $A_2 > 0$ has to be satisfied to guarantee the existence of E_1. According to Theorem 2.2, E_1 is always a saddle.

2.2.3. Hopf bifurcation near the non-trivial equilibrium E_1

Next, suppose that $A_2 < 0$ and $\rho < 0$ hold, so E_1 is stable as $\tau = 0$. As $\gamma^2 - \rho\gamma + S_1 \neq 0$, equation (2.21) becomes

$$(\gamma^2 - \rho\gamma + S_1)[\theta + (1 - \theta)e^{-\gamma\tau}] = 0. \tag{2.23}$$

Taking θ as the bifurcation parameter, for the equation

$$\theta + (1 - \theta)e^{-\gamma\tau} = 0,$$

its roots can be given by

$$\gamma_k = \frac{1}{\tau}(\ln(\frac{-(1 - \theta)}{\theta}) + 2k\pi i), \ k = 0, \ \pm 1, \ \pm 2, \cdots .$$

As $|\frac{-(1-\theta)}{\theta}| > 1$, which is equivalent to $0 < \theta < 0.5$, then the real part of $\ln(\frac{-(1-\theta)}{\theta})$ is positive, that is, $\mathrm{Re}(\ln(\frac{-(1-\theta)}{\theta})) = \ln|\frac{1-\theta}{\theta}| > 0$. By book [14], as $\theta < 0.5$, for all $\tau > 0$, there are an infinite number of roots of (2.21), whose real parts are positive. Furthermore, the equilibrium of system (2.19) is unstable for all $\tau > 0$.

For equation (2.21), it can be rewritten as

$$\gamma^2 + (\frac{1-\theta}{\theta})\gamma^2 e^{-\gamma\tau} + R(\gamma,\ \tau) = 0, \tag{2.24}$$

where $R(\gamma,\ \tau) = -(\frac{1-\theta}{\theta})\rho\gamma e^{-\gamma\tau} + (\frac{1-\theta}{\theta})S_1 e^{-\gamma\tau} - \rho\gamma + S_1$.

We consider

$$V(\gamma,\ \tau) = 1 + (\frac{1-\theta}{\theta})e^{-\gamma\tau} + \frac{R(\gamma,\ \tau)}{\gamma^2}, \gamma \neq 0.$$

Clearly, $V(\gamma,\ \tau)$ is analytic as $\gamma \neq 0$. By [14], if $\theta < 0.5$, there are $\mathrm{Re}(\gamma) > 0$ and $\frac{R(\gamma,\ \tau)}{\gamma^2} = 0$ as $|\gamma| \to \infty$, then there is a sequence of roots $\{\gamma_j\}$ of equation (2.24) such that $|\gamma_j| \to \infty$, and as $\tau \neq 0,\ j \to \infty$, $\mathrm{Re}(\gamma_\mathrm{j}) = \ \frac{1}{\tau}\ln|\frac{\theta-1}{\theta}| > 0$.

One can deduce the other case. As $|\frac{-(1-\theta)}{\theta}| < 1$, which is equivalent to $\theta > 0.5$, then $\mathrm{Re}(\ln(\frac{-(1-\theta)}{\theta})) = \ln|\frac{1-\theta}{\theta}| < 0$. By a similar way, as $\theta > 0.5$, for all $\tau > 0$, there are an infinite number of roots of (2.21), whose real parts are negative. Furthermore, the equilibrium of system (2.19) is stable for all $\tau > 0$. Moreover, one can see that the bifurcation point is $\theta = 0.5$ and

$$\gamma_k\ |_{\theta=0.5} = \frac{2k\pi i}{\tau},\quad \frac{d\mathrm{Re}(\gamma_\mathrm{k})}{d\theta}\ |_{\theta=0.5} = \frac{1}{\tau\theta(\theta-1)}\ |_{\theta=0.5} = -\frac{4}{\tau} \neq 0,\ k = 0,\ \pm1,\ \pm2, \cdots.$$

Theorem 2.3. *Assume that $a_1 > b$, $A_1A_2 > 0$ and $A_2 < 0$, $\rho < 0$ are satisfied. If $0 < \theta < 0.5$ $(1 > \theta > 0.5)$, then the equilibrium $E_1(k_1^*,\ p_{m1}^{0*})$ of the linear neutral delay differential system (2.17) is unstable (stable) for all $\tau > 0$. As $\theta = 0.5$, $\mathrm{Re}(\gamma) = 0$, which means the appearance of pure imaginary roots of the characteristic equation, E_1 is a Non-hyperbolic equilibrium, and there is a Hopf bifurcation near E_1.*

2.3. Decentralized decision-making model

Under decentralized decision making, the decision sequence of Stackelberg game is as follows. The manufacturer first decides the unit production cost $c_0 > 0$, the level of green technology $k(t)$, the market wholesale price $\omega(t) > 0$ and the online sale price $p_m^0(t)$. After receiving the manufacturer's decision information, the retailer decides its unit market sales price $p_r^0(t)$. $\Pi_m^d(t)$ and $\Pi_r^d(t)$ denote separately the instantaneous profit function of the manufacturer and retailer. From assumptions of Subsection 2.1, we have

$$\begin{aligned}\Pi_m^d(t) =&(p_m^0(t) - c_0)[\mu a - a_1 p_m^0(t) + a_2 g(t) + b p_r^0(t)]\\ &+ (\omega(t) - c_0)[(1-\mu)a - a_1 p_r^0(t) + a_2 g(t) + b p_m^0(t)] - \alpha k^2(t)/2,\\ \Pi_r^d(t) =&(p_r^0(t) - \omega(t))[(1-\mu)a - a_1 p_r^0(t) + a_2 g(t) + b p_m^0(t)].\end{aligned} \tag{2.25}$$

The manufacturer must first decide $k(t)$, $\omega(t)$ and $p_m^0(t)$. So the optimal market price of goods $p_r^0(t)$ needs to be found. Moreover, $\partial^2\Pi_r^d(t)/\partial p_r^{0^2}(t) = -2a_1 < 0$. Therefore, make $\partial\Pi_r^d(t)/\partial p_r^0(t) = 0$, namely,

$$\partial\Pi_r^d(t)/\partial p_r^0(t) = (1-\mu)a - 2a_1 p_r^0(t) + a_2 g(t) + b p_m^0(t) + a_1\omega(t) = 0. \tag{2.26}$$

From equation (2.26), one can deduce that

$$p_r^0(t) = \frac{(1-\mu)a + a_2 g(t) + b p_m^0(t) + a_1 \omega(t)}{2a_1}. \tag{2.27}$$

Replacing $p_r^0(g(t),\ \omega(t),\ p_m^0(t))$ into $p_r^0(t)$ of equation (2.25), there is

$$\begin{aligned}\Pi_m^d(t) =&(\omega(t) - c_0)[\frac{(1-\mu)}{2}a + \frac{b}{2}p_m^0(t) + \frac{a_2}{2}g(t) - \frac{a_1}{2}\omega(t)] - \frac{\alpha}{2}k^2(t)\\ &+ (p_m^0(t) - c_0)[\frac{[2a_1\mu + b(1-\mu)]a}{2a_1} + \frac{(b^2 - 2a_1^2)}{2a_1}p_m^0(t) + \frac{a_2(2a_1+b)}{2a_1}g(t) + \frac{b}{2}\omega(t)].\end{aligned}$$

Similarly, the present value of $\Pi_m^d(t)$ needs to be maximized, and the objective function can be derived, which is

$$\begin{aligned}&\max \int_0^{+\infty} e^{-\rho t}\ \Pi_m^d(t)dt\\ &s.t.\ g'(t) = k(t) - \delta g(t).\end{aligned}$$

The associated current value Hamilton function is

$$H_d(t) = \Pi_m^d(t) + e^{\rho t}\lambda(t)g'(t).$$

The economic meanings of $m(t)$, ρ, and $\lambda(t)$ remain the same. The necessary conditions for maximizing $H_d(t)$ can be given by

$$m'(t) = (\rho + \delta)m(t) - \frac{a_2[a_1\omega(t) + (2a_1+b)p_m^0(t) - (3a_1+b)c_0]}{2a_1}, \tag{2.28}$$

$$\frac{\partial H_d(t)}{\partial \omega(t)} = \frac{2bp_m^0(t) - 2a_1\omega(t) + a_2 g(t) + (1-\mu)a + (a_1 - b)c_0}{2} = 0, \tag{2.29}$$

$$\begin{aligned}\frac{\partial H_d(t)}{\partial p_m^0(t)} =& \frac{2(b^2 - 2a_1^2)p_m^0(t) + 2a_1 b\omega(t) + a_2(b+2a_1)g(t)}{2a_1}\\ &+ \frac{[2a_1\mu + b(1-\mu)]a + (a_1 - b)(2a_1+b)c_0}{2a_1}\\ =& 0,\end{aligned} \tag{2.30}$$

$$\frac{\partial H_d(t)}{\partial k(t)} = m(t) - \alpha k(t) = 0,\ k(t) = \frac{m(t)}{\alpha},\ k'(t) = \frac{m'(t)}{\alpha}. \tag{2.31}$$

From equations (2.29) and (2.30), the same as in the centralized model, we only focus on $a_1 > b$, and there are

$$p_m^0(t) = \frac{a_2}{2(a_1 - b)}g(t) + \frac{[a_1\mu + b(1-\mu)]a}{2(a_1^2 - b^2)} + \frac{c_0}{2}, \tag{2.32}$$

$$\omega(t) = \frac{a_2}{2(a_1 - b)}g(t) + \frac{[b\mu + a_1(1-\mu)]a}{2(a_1^2 - b^2)} + \frac{c_0}{2}, \tag{2.33}$$

$$\omega(t) = p_m^0(t) - \frac{(2\mu - 1)a}{2(a_1 + b)}. \tag{2.34}$$

By equation (2.32), there is

$$\frac{dp_m^0(t)}{dt} = \theta\frac{dp_m(t)}{dt} + (1-\theta)\frac{dp_m(t-\tau)}{dt} = \frac{a_2 g'(t)}{2(a_1-b)} = \frac{a_2}{2(a_1-b)}(k(t)-\delta g(t)).$$

Combining equations (2.28), (2.31) and (2.34), one can obtain

$$k'(t) = (\rho+\delta)k(t) - \frac{a_2(3a_1+b)}{2\alpha a_1}p_m^0(t) + \frac{a_2(3a_1+b)c_0}{2\alpha a_1} + \frac{(2\mu-1)a_1a_2a}{4\alpha a_1(a_1+b)}.$$

By equation (2.32), we obtain the following neutral delay differential system about $k(t)$ and $p_m(t)$:

$$\begin{cases} \dfrac{dk(t)}{dt} = (\rho+\delta)k(t) - \dfrac{a_2(3a_1+b)}{2\alpha a_1}\theta p_m(t) - \dfrac{a_2(3a_1+b)}{2\alpha a_1}(1-\theta)p_m(t-\tau) \\ \qquad\qquad + \dfrac{a_2(3a_1+b)c_0}{2\alpha a_1} + \dfrac{(2\mu-1)a_1a_2a}{4\alpha a_1(a_1+b)}, \\ \theta\dfrac{dp_m(t)}{dt} + (1-\theta)\dfrac{dp_m(t-\tau)}{dt} = \dfrac{a_2}{2(a_1-b)}k(t) - \delta\theta p_m(t) - \delta(1-\theta)p_m(t-\tau) \\ \qquad\qquad\qquad\qquad + \dfrac{[a_1\mu+b(1-\mu)]\delta a}{2(a_1^2-b^2)} + \dfrac{\delta c_0}{2}. \end{cases} \tag{2.35}$$

2.3.1. Existence of equilibrium for the system (2.35)

The corresponding ordinary differential equation can be obtained as follows:

$$\begin{cases} \dfrac{dk(t)}{dt} = (\rho+\delta)k(t) - \dfrac{a_2(3a_1+b)}{2\alpha a_1}p_m^0(t) + \dfrac{a_2(3a_1+b)c_0}{2\alpha a_1} + \dfrac{(2\mu-1)a_1a_2a}{4\alpha a_1(a_1+b)}, \\ \dfrac{dp_m^0(t)}{dt} = \dfrac{a_2}{2(a_1-b)}k(t) - \delta p_m^0(t) + \dfrac{[a_1\mu+b(1-\mu)]\delta a}{2(a_1^2-b^2)} + \dfrac{\delta c_0}{2}. \end{cases}$$

By the same way as in the system (2.17), we can get the existence of a positive equilibrium.

Theorem 2.4. *If the parameters satisfy*

$$B_1B_2 > 0,\ a_1 > b,$$

where

$$B_1 = a_2\big([(a_1-b)\mu+(a_1+b)]a + (b-a_1)(3a_1+b)c_0\big),\ B_2 = 4\alpha a_1\delta(\rho+\delta)(a_1-b) - a_2^2(3a_1+b),$$

then there is a unique positive equilibrium $E_2(k_2^*,\ p_{m2}^{0*})$, and

$$p_{m2}^{0*} = \frac{a_2B_1}{2(a_1-b)B_2} + \frac{[a_1\mu+b(1-\mu)]a}{2(a_1^2-b^2)} + \frac{c_0}{2},\ k_2^* = \frac{\delta B_1}{B_2}.$$

As the system is in equilibrium, if

$$a > \max\{\frac{(2a_1+b)[(a_1-b)c_0 - a_2g_2^*]}{2a_1\mu+b(1-\mu)},\ \frac{(a_1+b)[(a_1-b)c_0-a_2g_2^*]}{a_1\mu+b(1-\mu)}\},$$

by equations (2.2), (2.3), (2.27), (2.31), (2.32), and (2.33), then we can get other values as follows:

$$p_{r2}^{0*} = \frac{a_2(3a_1-b)B_1}{4a_1(a_1-b)B_2} + \frac{[2a_1b\mu + (3a_1^2-b^2)(1-\mu)]a}{4a_1(a_1^2-b^2)} + \frac{(a_1+b)c_0}{4a_1},$$
$$g_2^* = \frac{B_1}{B_2},\ m_2^* = \alpha k_2^*,\ D_{m2}^* = \frac{a_2(2a_1+b)B_1}{4a_1B_2} + \frac{[2a_1\mu + b(1-\mu)]a}{4a_1} + \frac{(2a_1+b)(b-a_1)c_0}{4a_1},$$
$$\omega^* = \frac{a_2B_1}{2(a_1-b)B_2} + \frac{[b\mu + a_1(1-\mu)]a}{2(a_1^2-b^2)} + \frac{c_0}{2},\ D_{r2}^* = \frac{a_2B_1}{4B_2} + \frac{[a_1\mu + b(1-\mu)]a}{4(a_1+b)} + \frac{(b-a_1)c_0}{4}.$$

2.3.2. Stability of equilibrium for the system (2.35)

By doing a similar transformation, there is

$$\begin{cases} \dfrac{dk(t)}{dt} = (\rho+\delta)k(t) - \dfrac{a_2(3a_1+b)}{2\alpha a_1}\theta p_m(t) - \dfrac{a_2(3a_1+b)}{2\alpha a_1}(1-\theta)p_m(t-\tau), \\ \theta\dfrac{dp_m(t)}{dt} + (1-\theta)\dfrac{dp_m(t-\tau)}{dt} = \dfrac{a_2}{2(a_1-b)}k(t) - \delta\theta p_m(t) - \delta(1-\theta)p_m(t-\tau). \end{cases} \tag{2.36}$$

Substituting $k(t) = e^{\chi t}\varsigma,\ p_m(t) = e^{\chi t}\phi$ into (2.36), χ and (ς, ϕ) are separately the eigenvalue and eigenvector of the corresponding characteristic equation. One can obtain the characteristic matrix equation, which is

$$\begin{bmatrix} \chi - (\rho+\delta)\dfrac{a_2(3a_1+b)\theta}{2\alpha a_1} + \dfrac{a_2(3a_1+b)(1-\theta)}{2\alpha a_1}e^{-\chi\tau} \\ -\dfrac{a_2}{2(a_1-b)}\theta\chi + (1-\theta)\chi e^{-\chi\tau} + \delta\theta + \delta(1-\theta)e^{-\chi\tau} \end{bmatrix} \begin{bmatrix} \varsigma \\ \phi \end{bmatrix} = 0.$$

So the characteristic equation is

$$[\theta + (1-\theta)e^{-\chi\tau}]\big\{(\chi+\delta)[\chi-(\rho+\delta)] + \frac{a_2^2(3a_1+b)}{4\alpha a_1(a_1-b)}\big\} = 0. \tag{2.37}$$

Equation (2.37) becomes a second-degree exponential polynomial equation

$$(\chi^2 - \rho\chi + S_2)\theta + (1-\theta)(\chi^2 - \rho\chi + S_2)e^{-\chi\tau} = 0, \tag{2.38}$$

where

$$S_2 = \frac{a_2^2(3a_1+b) - 4\alpha a_1\delta(\rho+\delta)(a_1-b)}{4\alpha a_1(a_1-b)} = \frac{-B_2}{4\alpha a_1(a_1-b)}.$$

As $\theta = 1$ or $\tau = 0$, the corresponding characteristic equation is

$$\chi^2 - \rho\chi + S_2 = 0.$$

Similarly to equation (2.22), we can obtain the following results.

Theorem 2.5. *Assume that $B_1B_2 > 0$ is satisfied. The following results hold.*

(1) *If $B_2 > 0$, then E_2 is a saddle.*

(2) *If $B_2 < 0,\ \rho > 0$ and $B_2 + \rho^2\alpha a_1(a_1-b) > 0\ (< 0)$, then E_2 is an unstable node (focus).*

(3) *If* $B_2 < 0,\ \rho < 0$ *and* $B_2 + \rho^2\alpha a_1(a_1 - b) > 0\ (< 0)$*, then* E_2 *is an asymptotically stable node (focus).*

(4) *If* $B_2 < 0,\ \rho = 0$*, then* E_2 *is the center of system (2.35).*

Remark 2.6. When $\theta = 0$, the corresponding case is that we only consider the case of making decisions with reference to the historical time-delay parameter. The reason for this situation is that enterprises sometimes lag behind in grasping market information when making decisions, and it is difficult to obtain the current market price accurately and timely.

2.3.3. Hopf bifurcation near the non-trivial equilibrium E_2

As $\chi^2 - \rho\chi + S_2 \neq 0, \tau \neq 0$, equation (2.38) becomes

$$(\chi^2 - \rho\chi + S_2)[\theta + (1 - \theta)e^{-\chi\tau}] = 0. \tag{2.39}$$

Equation (2.39) is similar to equation (2.23), after a similar prove process of Hopf bifurcation near the non-trivial equilibrium E_1, we can obtain the following theorem.

Theorem 2.6. *Assume that* $a_1 > b,\ B_1B_2 > 0$ *and* $B_2 < 0,\ \rho < 0$ *are satisfied. If* $0 < \theta < 0.5\ (1 > \theta > 0.5)$*, then the equilibrium* E_2 *of the linear neutral delay differential system (2.36) is unstable (stable) for all* $\tau > 0$*. As* $\theta = 0.5$*, there is the appearance of pure imaginary roots of the characteristic equation. Namely, Hopf bifurcation appears near* E_2*.*

3. Optimal decision analysis: A cooperative coordination model

In Subsections 2.2.1 and 2.3.1, the optimal green technology level and the optimal price have been obtained in two decision making situations. Next, by conducting a comparative analysis, we have the following results.

Theorem 3.1. *Suppose that* $A_1A_2 > 0,\ a_1 > b$ *and* $B_1B_2 > 0$ *are satisfied. If* $1 - 2\mu > 0$ *and* $B_2 > 0$*, then the optimal green technology levels, greenness of the product and best sale prices of two decision making situations satisfy* $k_1^* > k_2^*,\ g_1^* > g_2^*,\ p_{m1}^* > p_{m2}^*$ *and* $p_{r1}^* > \omega^*$*.*

Proof. If the parameters satisfy $1 - 2\mu > 0$ and $B_2 > 0$, one can deduce that

$$g_1^* - g_2^* = \frac{A_1}{A_2} - \frac{B_1}{B_2} = \frac{\alpha\delta(\rho + \delta)(a_1 - b)^2A_1}{A_2B_2} + \frac{a_2(1 - 2\mu)(a_1 - b)a}{2B_2} > 0,$$

then $g_1^* > g_2^*$. Hence, $k_1^* > k_2^*,\ p_{m1}^* > p_{m2}^*,\ p_{r1}^* > \omega^*$. The proof is finished. □

When $A_1A_2 > 0$ is satisfied, the maximum total profit Π^{c*} can be got

$$\Pi^{c*} = [p_{m1}^{0*} - c_0]D_{m1}^* + [p_{r1}^{0*} - c_0]D_{r1}^* - \alpha k_1^{*2}/2.$$

As $B_1B_2 > 0$ and $a_1 > b$ are satisfied, the maximum manufacturer profit Π_m^d and retailer profit Π_r^d can be obtained as follows:

$$\Pi_m^{d*} = (p_{m2}^{0*} - c_0)D_{m2}^* + (\omega^* - c_0)D_{r2}^* - \alpha k_2^{*2}/2, \quad \Pi_r^{d*} = (p_{r2}^{0*} - \omega^*)D_{r2}^*.$$

If $\Pi^{c*} > \Pi^{d*} = \Pi_m^{d*} + \Pi_r^{d*}$ $(\Pi^{c*} < \Pi^{d*} = \Pi_m^{d*} + \Pi_r^{d*})$, then the total profit of dual channel GSCs in centralized decision-making circumstance will be higher (lower) than that of the decentralized decision-making condition.

Table 1. The description of arguments and the related values used in numerical simulations.

Parameter	Descriptions	Values
a	Total market demand	100
a_2	Consumer sensitivity to $g(t)$	0.4
α	Green investment cost coefficient	5
δ	The decline coefficient of $g(t)$	0.3
c_0	The unit cost	5
ρ	The discount rate	0.1
a_1	The price sensitivity	1.2
b	Two channel cross price elasticity coefficient	0.4
μ	Initial market share of e-direct channels	0.7

As the parameter group values choose the values of Table 1, we can get $\Pi^{c*} > \Pi^{d*}$, which is shown in Table 2. The result in Table 2 shows that the total profit of the decentralized

Table 2. Profit comparisons of two decision systems.

Π_m^{d*}	Π_r^{d*}	Π^{d*}	Π^{c*}
6602.4	796.4	7398.8	15338

dual channel GSCs is not optimal. However, for centralized decision-making dual channel GSCs members, making a unified strategy is still difficult. Therefore, to further GSCs members cooperate and converge to the optimal profit of the centralized control dynamic model, we need to design a cooperative coordination model.

To eliminate the double marginalization effect and achieve Pareto improvement for all supply chain participants, a transfer payment mechanism independent of the wholesale price is proposed. The core idea is to guide the decentralized supply chain to achieve the first-best performance identical to the centralized scenario, and then redistribute the increased total profit through a fixed transfer payment ν to ensure that both the manufacturer and the retailer obtain no less profit than in the decentralized scenario. Under the coordination mechanism, the retail prices, demands, green degree, and green investment are set to the centralized optimal values:

$$p_m^{co} = p_{m1}^{0*}, \quad p_r^{co} = p_{r1}^{0*}, \quad D_m^{co} = D_{m1}^*, \quad D_r^{co} = D_{r1}^*, \quad g^{co} = g_1^*, \quad k^{co} = k_1^*,$$

where $p_{m1}^{0*}, p_{r1}^{0*}, D_{m1}^*, D_{r1}^*, g_1^*, k_1^*$ are the centralized equilibrium values defined in Theorem 2.1.

The total supply chain profit under coordination is exactly equal to the centralized total profit:

$$\Pi^{co} = \Pi^{c*} = (p_{m1}^{0*} - c_0)D_{m1}^* + (p_{r1}^{0*} - c_0)D_{r1}^* - \alpha k_1^{*2}/2.$$

The profits of the manufacturer and retailer under coordination (before redistribution) are:

$$\begin{cases} \Pi_m^{co,0} = (p_{m1}^{0*} - c_0)D_{m1}^* + (\omega^* - c_0)D_{r1}^* - \dfrac{1}{2}\alpha(k_1^*)^2, \\ \Pi_r^{co,0} = (p_{r1}^{0*} - \omega^*)D_{r1}^*, \end{cases}$$

where ω^* is the wholesale price under decentralized decision-making.

A fixed transfer payment ν ($\nu =\mid \Pi^{d*} - \Pi_m^{co,0} \mid \times 0.8$) is introduced to redistribute the profit, ensuring Pareto improvement:

$$\begin{cases} \Pi_m^{co} = \Pi_m^{co,0} - \nu, \\ \Pi_r^{co} = \Pi_r^{co,0} + \nu, \end{cases}$$

where Π^{d*} is the total profit under decentralized decision-making, calculated from the decentralized equilibrium $E_2(k_2^*, p_{m2}^{0*})$.

The performance of the coordination mechanism is verified through numerical experiments. The parameter settings are consistent with the previous analysis, and the results are summarized in Table 3.

Table 3. Profit comparison between decentralized and coordinated scenarios.

Profit Type	Decentralized	Coordinated
Total Supply Chain Profit	7398	15338 (First-best)
Manufacturer's Profit	6602.4	7981.3
Retailer's Profit	796.4	7356.4

Using the parameter values listed in Table 1, we first verify the efficiency loss in the decentralized scenario, as shown in Table 2. The total supply chain profit under decentralized decision-making is $\Pi^{d*} = 7398.8$, which is significantly lower than the first-best centralized total profit $\Pi^{c*} = 15338$, indicating the existence of double marginalization effect.

To eliminate this inefficiency and achieve Pareto improvement, we implement the transfer payment mechanism, and the results are summarized in Table 3. It can be observed that:

- The total supply chain profit under coordination rises to $\Pi^{co} = 15338$, which is exactly identical to the centralized total profit, demonstrating that the coordination mechanism successfully achieves the first-best performance and completely eliminates the efficiency loss.
- The manufacturer's profit increases from $\Pi_m^{d*} = 6602.4$ to $\Pi_m^{co} = 7981.3$, representing a growth of 20.88%, while the retailer's profit slightly increases from $\Pi_r^{d*} = 796.4$ to $\Pi_r^{co} = 7356.4$, a growth of 823.71%.
- Both participants obtain higher profits than in the decentralized scenario, realizing a strict Pareto improvement.

This comparison confirms that the proposed coordination mechanism not only enhances the overall supply chain efficiency but also ensures a win-win outcome for all members, which validates the effectiveness and practicality of the mechanism in green dual-channel supply chains.

To evaluate the effectiveness of the coordination mechanism comprehensively, we provide a performance comparison among the centralized, decentralized, and coordinated scenarios. The coordinated scenario is designed to achieve the centralized optimal performance by using a transfer payment contract that ensures Pareto improvement for both players.

The profit forms under coordination are consistent with the equilibrium structure of the system, and the transfer payment ν is determined to ensure $\Pi_m^{co} \geq \Pi_m^{d*}$ and $\Pi_r^{co} \geq \Pi_r^{d*}$. The performance indicators include total supply chain profit, greenness level, green investment, and individual profits of the manufacturer and retailer.

To comprehensively evaluate the effectiveness of the coordination mechanism, we provide a performance comparison among the centralized, decentralized, and coordinated scenarios, covering both economic efficiency and environmental sustainability. The results are summarized in Table 4.

Table 4. Performance comparison among centralized, decentralized, and coordinated scenarios.

Index	Centralized	Decentralized	Coordinated
Total profit Π^*	15538	7398.8	15538
Greenness g^*	442.3	244.1	442.3
Green investment k^*	79.6	43.9	79.6
Manufacturer profit Π_m^*	—	6602.4	7981.3
Retailer profit Π_r^*	—	796.4	7356.4

From Table 4, we observe that:

- The total supply chain profit under coordination reaches the first-best level of the centralized scenario, completely eliminating the double marginalization effect.
- The greenness level g^* and green investment k^* under coordination are optimized to the centralized optimal values (442.3 and 79.6, respectively), which are significantly higher than those under decentralization (244.1 and 43.9), demonstrating improved environmental sustainability.
- Both the manufacturer and retailer obtain strictly higher profits under coordination than in the decentralized scenario, ensuring a win-win outcome for all supply chain members.

4. Sensitivity analysis

By computing, we can analyze the influences of the consumer sensitivity to the greenness of the product a_2, the total market demand a, the green investment cost coefficient α, the decline coefficient function of the greenness of the product δ, the discount rate ρ, the price sensitivity a_1, the two channel cross price elasticity coefficient b and the unit production cost c_0 on the equilibrium. By Table 5, for E_1 (E_2), we know that both k_1^* (k_2^*) and p_{m1}^{0*} (p_{m2}^{0*}) are positively related to the greenness of the product g_1^* (g_2^*) based on $A_1A_2 > 0$ ($B_1B_2 > 0$). Therefore, we

Table 5. Expressions of A_1, A_2 g_1^*, k_1^*, p_{m1}^*, p_{r1}^* and B_1, B_2, g_2^*, k_2^*, p_{m2}^*, p_{r2}^*, ω^*.

Parameter	Expression	Parameter	Expression
A_1	$a_2[a+2(b-a_1)c_0]$	B_1	$a_2\big([(a_1-b)\mu+(a_1+b)]a+(b-a_1)(3a_1+b)c_0\big)$
A_2	$2[\alpha\delta(\rho+\delta)(a_1-b)-a_2^2]$	B_2	$4\alpha a_1\delta(\rho+\delta)(a_1-b)-a_2^2(3a_1+b)$
g_1^*	$\dfrac{A_1}{A_2}$	g_2^*	$\dfrac{B_1}{B_2}$
k_1^*	$\dfrac{\delta A_1}{A_2}$	k_2^*	$\dfrac{\delta B_1}{B_2}$
p_{m1}^{0*}	$\dfrac{a_2A_1}{2(a_1-b)A_2}+\dfrac{[a_1\mu+b(1-\mu)]a}{2(a_1^2-b^2)}+\dfrac{c_0}{2}$	p_{m2}^{0*}	$\dfrac{a_2B_1}{2(a_1-b)B_2}+\dfrac{[a_1\mu+b(1-\mu)]a}{2(a_1^2-b^2)}+\dfrac{c_0}{2}$
p_{r1}^{0*}	$\dfrac{a_2A_1}{2(a_1-b)A_2}+\dfrac{[b\mu+a_1(1-\mu)]a}{2(a_1^2-b^2)}+\dfrac{c_0}{2}$	p_{r2}^{0*}	$\dfrac{a_2(3a_1-b)B_1}{4a_1(a_1-b)B_2}+\dfrac{[2a_1b\mu+(3a_1^2-b^2)(1-\mu)]a}{4a_1(a_1^2-b^2)}+\dfrac{(a_1+b)c_0}{4a_1}$
		ω^*	$\dfrac{a_2B_1}{2(a_1-b)B_2}+\dfrac{[b\mu+a_1(1-\mu)]a}{2(a_1^2-b^2)}+\dfrac{c_0}{2}$

can investigate the effects of these parameters on g_1^* (g_2^*) as follows.

4.1. Local sensitivity analysis

Notice that δ is the decline coefficient function of the greenness of the product, so δ is negatively related to k_1^* (k_2^*) and p_{m1}^{0*} (p_{m2}^{0*}). Under the centralized decision making, we have the following cases.

(I) The signs of $\partial g_1^*/\partial a_2$ and $g_1^*/\partial a$ are the same as those of A_1 and A_2, because

$$\frac{\partial g_1^*}{\partial a_2} = \frac{[\alpha\delta(\rho+\delta)(a_1-b)+a_2^2]A_1}{a_2A_2^2},\ \frac{\partial g_1^*}{\partial a} = \frac{a_2}{A_2}.$$

Recall that $A_1A_2 > 0$, which means that the signs of A_1 and A_2 are the same. So the effects of parameter a_2, a on g_1^* are similar. If $A_2 > 0$, then $g_1^*/\partial a_2 > 0$, $\partial g_1^*/\partial a > 0$, g_1^* increases as a_2 or a increases. In other words, when the consumer's sensitivity to the greenness of the product increases or the total market demand expands, the greenness of the product will increase. If $A_2 < 0$, then g_1^* decreases as a_2 or a increases. Namely, as the consumer's sensitivity to the greenness of the product increases or the total market demand expands, the greenness of the product will decrease.

(II) Because

$$\frac{\partial g_1^*}{\partial \alpha} = \frac{-2\delta(\rho+\delta)(a_1-b)A_1}{A_2^2},\ \frac{\partial g_1^*}{\partial \rho} = \frac{-2\alpha\delta(a_1-b)A_1}{A_2^2},\ \frac{\partial g_1^*}{\partial c_0} = \frac{-2a_2(a_1-b)}{A_2},$$

the signs of $\partial g_1^*/\partial\alpha$ and $\partial g_1^*/\partial\rho$ are opposite to that of A_1 and the sign of $\partial g_1^*/\partial c_0$ is opposite to that of A_2. Thus, parameters α, ρ, c_0 have similar impacts on g_1^*. If $A_1 > 0$ ($A_1 < 0$), then g_1^* decreases (grows) as α, ρ or c_0 increases. That is, the greenness of the product will decrease (increase) as the green investment cost coefficient α, the discount rate ρ or the unit production cost c_0 increases.

(III) The effects of a_1 and b on g_1^* are different from the others. It is irrelevant to the sigh of A_1 or A_2, but only depends on the sign of $\alpha\delta(\rho+\delta)a - 2a_2^2c_0$, which is because

$$\frac{\partial g_1^*}{\partial a_1} = \frac{-2a_2[\alpha\delta(\rho+\delta)a-2a_2^2c_0]}{A_2^2},\ \frac{\partial g_1^*}{\partial b} = \frac{2a_2[\alpha\delta(\rho+\delta)a-2a_2^2c_0]}{A_2^2}.$$

Moreover, we can see that the trend of a_1 and b about g_1^* is exactly opposite. That is, if $\alpha\delta(\rho+\delta)a - 2a_2^2c_0 > 0$ (< 0), then g_1^* declines (grows) as b is reducing or a_1 is rising. Equivalently, the greenness of the product declines (grows) as the price sensitivity increases or the two channel cross price elasticity coefficient decreases.

Summarizing the above analysis, we can obtain the following theorem.

Theorem 4.1. *Assume that $A_1A_2 > 0$, $a_1 > b$.*

(i) If $A_1 > 0$, then g_1^* goes up as a_2 or a increases, and g_1^* decreases as α, ρ or c_0 is on the rise. If $A_1 < 0$, then g_1^* goes down as a_2 or a rises, and g_1^* grows as α, ρ or c_0 is on the increase; So to speak, if $A_1 > 0$ ($A_1 < 0$), the greenness of the product will increase (decrease) when the consumer's sensitivity to the greenness of the product increases or the total market demand expands. While the greenness of the product will decrease (increase) as the green investment cost coefficient α, the discount rate ρ or the unit production cost c_0 greenness increases.

(ii) If $\alpha\delta(\rho+\delta)a - 2a_2^2c_0 > 0$, then g_1^* declines as b reduces or a_1 enhances. If $\alpha\delta(\rho+\delta)a - 2a_2^2c_0 < 0$, then g_1^* grows as b decreases or a_1 increases. In other words, if $\alpha\delta(\rho+\delta)a - 2a_2^2c_0 > 0$ ($\alpha\delta(\rho+\delta)a - 2a_2^2c_0 < 0$), the greenness of the product declines (grows) as the price sensitivity increases or the two-channel cross-price elasticity coefficient decreases.

In order to show it more intuitively, for the centralized model (2.18), by Theorem 4.1, the influence table of parameters on g_1^* can be included as follows.

Table 6. The influence of parameters on g_1^*.

	a_2	a	α	c_0	ρ	b	a_1
$A_1 > 0$	↑	↑	↓	↓	↓		
$A_1 < 0$	↓	↓	↑	↑	↑		
$\alpha\delta(\rho+\delta)a - 2a_2^2c_0 > 0$						↑	↓
$\alpha\delta(\rho+\delta)a - 2a_2^2c_0 < 0$						↓	↑

Remark 4.1. Differently from the sensitivity analysis method studied in [23], we use the continuous derivative method rather than the discontinuous list method, which can directly see the continuous influence of each parameter on the positive equilibrium in detail.

Next, we can also study these parameters (except δ) how they affect directly g_2^* and indirectly $E_2(k_2^*,\ p_{m2}^{0*})$ under the decentralized decision making based on $B_1B_2 > 0$, which can concluded as follows.

(I) Let $\eta = 4a_1\alpha\delta(\rho+\delta)$, then $\eta > 0$. The signs of $\partial g_2^*/\partial a_2$, $\partial g_2^*/\partial a$, $\partial g_2^*/\partial\mu$ and $\partial g_2^*/\partial b$ are the same as those of B_1 and B_2, respectively, because

$$\frac{\partial g_2^*}{\partial a_2} = \frac{B_1[\eta(a_1-b)+a_2^2(3a_1+b)]}{a_2B_2^2},\ \frac{\partial g_2^*}{\partial a} = \frac{a_2[(a_1-b)\mu+(a_1+b)]}{B_2},$$
$$\frac{\partial g_2^*}{\partial \mu} = \frac{(a_1-b)aa_2}{B_2},\ \frac{\partial g_2^*}{\partial b} = \frac{B_2a_2[(1-\mu)a+2(a_1+b)c_0]+B_1[\eta+a_2^2]}{B_2^2},$$

the influences of parameter $a_2,\ a,\ \mu,\ b$ on g_2^* are same. If $B_1 > 0$, then g_2^* goes up as $a_2,\ a,\ \mu$ or b increases. If $B_1 < 0$, then g_2^* goes down as $a_2,\ a,\ \mu$ or b rises.

(II) Let $\eta_1 = -4a_1(a_1-b)$, then $\eta_1 < 0$. Since

$$\frac{\partial g_2^*}{\partial \alpha} = \frac{\eta_1\delta(\rho+\delta)B_1}{B_2^2},\ \frac{\partial g_2^*}{\partial \rho} = \frac{\eta_1\alpha\delta B_1}{B_2^2},\ \frac{\partial g_2^*}{\partial c_0} = \frac{-a_2(3a_1+b)(a_1-b)}{B_2},$$

the signs of $\partial g_2^*/\partial\alpha$ and $\partial g_2^*/\partial\rho$ are opposite to that of B_1 and the sign of $\partial g_2^*/\partial c_0$ is opposite to that of B_2. Thus, the parameters $\alpha,\ \rho$, and c_0 have the similar impacts on g_2^*. If $B_1 > 0$, then g_2^* decreases as $\alpha,\ \rho$ or c_0 increases. If $B_1 < 0$, then g_2^* grows as $\alpha,\ \rho$ or c_0 is on the increase.

(III) The effect of a_1 on g_2^* is different from that of others. It is irrelevant to the sign of B_1 or B_2, which is because

$$\frac{\partial g_2^*}{\partial a_1} = \frac{a_2^3(3a_1+b)^2c_0 + 4\alpha\delta(\rho+\delta)(a_1-b)^2ba_2c_0}{B_2^2}$$
$$+ \frac{2a_2^3b(1-2\mu)a - 4a_2\alpha\delta(\rho+\delta)[a_1^2-b^2+2a_1b+(a_1-b)^2\mu]a}{B_2^2}.$$

Moreover, we can see that if $\mu > 0.5,\ a > a^*$ $(a < a^*)$, then g_2^* is negatively (positively) increasing about a_1, where

$$a^* = \frac{a_2^3(3a_1+b)^2c_0 + 4\alpha\delta(\rho+\delta)(a_1-b)^2ba_2c_0}{2a_2^3b(2\mu-1) + 4a_2\alpha\delta(\rho+\delta)[a_1^2-b^2+2a_1b+(a_1-b)^2\mu]}.$$

Thus, we can also summarize and get the following claim.

Theorem 4.2. *Assume that $B_1B_2 > 0,\ a_1 > b$.*

(i) If $B_1 > 0$, then g_2^* goes up as a_2, a, μ or b increases, and g_2^* decreases as α, ρ or c_0 is on the rise. If $B_1 < 0$, then g_2^* goes down as a_2, a, μ or b or a rises, and g_2^* grows as α, ρ or c_0 is on the increase; That is, if $B_1 > 0$ $(B_1 < 0)$, then the greenness of the product of the decentralized model will increase (decrease) when the consumer's sensitivity to the greenness of the product increases, the total market demand expands, the representative of the initial market share of electronic direct marketing channels enlarges or the two channel cross price elasticity coefficient grows larger. While the greenness of the product will decrease (increase) as the green investment cost coefficient α, the discount rate ρ or the unit production cost c_0 increases.

(ii) If $\mu > 0.5,\ a > a^*$ $(a < a^*)$, then the greenness of the product of the decentralized model g_2^* is negatively (positively) increasing about the price sensitivity a_1.

For the decentralized model (2.35), according to Theorem 4.2, the influence table of the parameters on g_2^* can be included as follows.

Table 7. The influence of parameters on g_2^*.

	a_2	a	α	c_0	ρ	b	μ	a_1
$B_1 > 0$	↑	↑	↓	↓	↓	↑	↑	
$B_1 < 0$	↓	↓	↑	↑	↑	↓	↓	
$\mu > 0.5,\ a > a^*$								↓
$\mu > 0.5,\ a < a^*$								↑

Remark 4.2. By comparative analysis, we can find that the trends of the optimal greenness of the product subject to a_2, a, α, ρ, c_0 and δ are same in two decision-making situations. Furthermore, the trend of k_2^* with regard to these parameters is the same as that of g_2^*. Meanwhile, by a similar method, the trends of p_{r2}^*, p_{m2}^*, D_{r2}^*, D_{m2}^* can also be obtained, which is omitted for the long formula and complex computation.

Local sensitivity analysis is typically only applicable near the equilibrium point and may not capture nonlinear interactions, so we proceed with a global sensitivity analysis next.

4.2. Global sensitivity analysis

While local sensitivity analysis provides valuable insights into parameter influences at equilibrium points, it lacks the capability to quantify the interactions among parameters and their collective impact on system outputs across the entire parameter space. To address this limitation, we employ the Sobol global sensitivity analysis method [30,32], which is based on variance decomposition and capable of evaluating both first-order and total-effect sensitivity indices.

The fundamental principle of the Sobol method involves the decomposition of the total variance of the output function $Y = f(X_1, X_2, \ldots, X_k)$ into partial variances attributable to individual parameters and their interactions:

$$V(Y) = \sum_{i=1}^{k} V_i + \sum_{i<j}^{k} V_{ij} + \cdots + V_{12\ldots k}, \tag{4.1}$$

where V_i represents the variance due to parameter X_i alone, V_{ij} denotes the variance due to interactions between X_i and X_j, and so on.

The first-order Sobol index S_i measures the main effect of the parameter X_i on the output variance:

$$S_i = \frac{V_i}{V(Y)}. \tag{4.2}$$

The total effect Sobol index S_{Ti} captures the overall contribution of parameter X_i, including all interactions with other parameters:

$$S_{Ti} = \frac{V_i + \sum_{j\neq i} V_{ij} + \cdots}{V(Y)} = 1 - \frac{V_{\sim i}}{V(Y)}, \tag{4.3}$$

where $V_{\sim i}$ represents the variance due to all parameters except X_i.

Lemma 4.1 (Sobol sensitivity indices properties)**.** *Let S_i and S_{Ti} denote separately the first-order and total-effect Sobol indices for the parameter X_i in the system output $Y = f(X_1, X_2, \ldots, X_k)$. Then the following properties hold:*

- $0 \leq S_i \leq S_{Ti} \leq 1$ *for all* $i = 1, 2, \ldots, k$.
- $-\sum_{i=1}^{k} S_i \leq 1 \leq \sum_{i=1}^{k} S_{Ti}$.
- *The interaction effect $I_i = S_{Ti} - S_i$ quantifies the total contribution of all interactions involving the parameter X_i* [32].

For our dual channel GSCS, we focus on the following key parameters that significantly influence the stability and performance of the system, and quantify their influence on two core system output metrics: Green technology level g^* and total profit Π^*. g^* reflects the environmental sustainability of the GSC system and Π^* captures the overall economic performance. These two metrics jointly characterize the dual bottom line of the green supply chain. We employ Latin Hypercube Sampling (LHS) [22] *to generate 10,000 combinations of parameters within specified ranges (Table 8), ensuring comprehensive coverage of the parameter space while maintaining computational efficiency. The choice of some parameters ranges are based on* [3, 23].

Table 8. Parameter ranges for global sensitivity analysis.

Parameter	Symbol	Minimum	Maximum	References
Discount rate	ρ	-0.75	0.2	[3, 23]
Consumer green sensitivity	a_2	0.03	0.12	[23]
Price weight coefficient	θ	0	1	Assumed
Time delay	τ	0	6	Assumed
Green investment cost coefficient	α	0.8	1.2	[23]
Unit production cost	c_0	0.008	0.015	[23]

The Sobol sensitivity indices for the key output metrics of system (green technology level g^* and total profit Π^*) are presented in Table 9 and visualized in Figure 1 (a) and Figure 1 (b).

Table 9. Sobol sensitivity indices for system output.

Parameter	First-order index (S_i)	Total-effect index (S_{Ti})	Ranking
ρ	0.4611	0.4701	1
a_2	0.3127	0.3187	2
θ	0.1075	0.1054	3
τ	0.0609	0.0626	4
α	0.024	0.0268	5
c_0	0.0134	0.0175	6

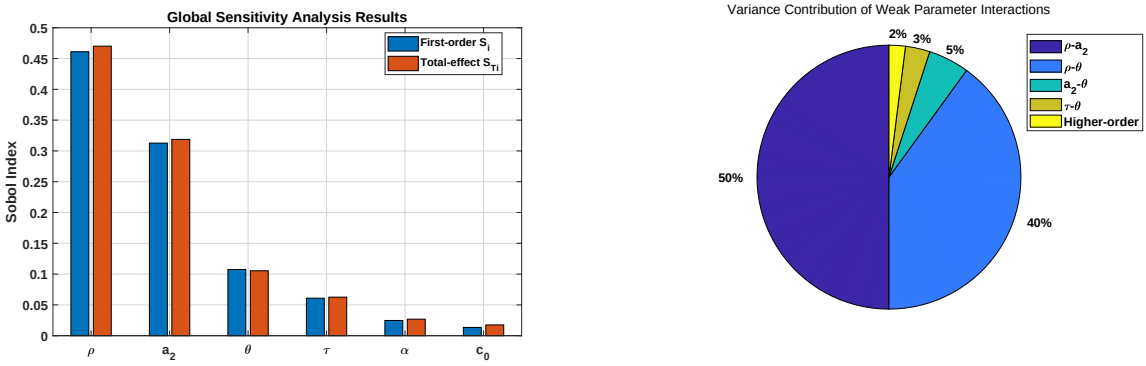

(a) First-order and total-effect Sobol indices for key parameters (b) Parameter interaction effect analysis pie chart

Figure 1. Global sensitivity analysis of key parameters in the dual channel green supply chain.

Corollary 4.1 (Parameter interaction effects)**.** *For the GSCS model, the small differences between the first-order indices (S_i) and total-effect indices (S_{Ti}) in Table 7 indicate that parameter interaction effects ($I_i = S_{Ti} - S_i$) are negligible. Specifically:*

- *The total interaction effect accounts for only about 2% of the output variance, confirming that parameter influences are largely independent.*
- *The strongest pairwise interaction (between ρ and a_2) contributes less than 1% to the total variance.*
- *Higher-order interactions collectively explain a negligible fraction of the output variance.*

Practically, despite weak interactions, managers should:

- *Align financial incentives (ρ) with green marketing (a_2) to capture residual synergies.*
- *Coordinate pricing (θ) and financial planning (ρ) to account for minor interaction effects.*
- *Maintain a holistic approach to parameter optimization for optimal system performance.*

Corollary 4.2 (Dominant parameter identification). *Based on Table 9 and Figure 1, consider the dual channel GSCS with parameters defined in Section 2. Under conditions $a_1 > b$ and $A_1 A_2 > 0$, the following ranking of parameter influence holds:*

$$\rho \succ a_2 \succ \theta \succ \tau \succ \alpha \succ c_0,$$

where $\succ$ denotes 'has greater influence than'. The detailed first-order and total-effect Sobol indices are summarized in Table 9.

Lemma 4.2 (Financial parameter dominance). *The discount rate ρ exhibits financial dominance in the system, satisfying:*

$$S_{T\rho} > \max(S_{Ta_2}, S_{T\theta}, S_{T\tau}, S_{T\alpha}, S_{Tc_0}).$$

This indicates that the influence of ρ is greater than any other single parameter.

Theorem 4.3 (Priority principle of financial parameters). *For optimal management of green supply chains under uncertainty, financial parameters should receive priority attention. Specifically:*

- *Monitoring and managing the discount rate ρ should be the primary focus, as it dominates system behavior ($S_{T\rho} = 0.4701$).*
- *Financial incentives and investment strategies should be designed considering ρ's profound impact on green technology investment decisions.*
- *The influence of the discount rate persists in both centralized and decentralized decision-making scenarios.*

Theorem 4.4 (Consumer's sensitivity leverage effect). *The green sensitivity of the consumer a_2 serves as the second most influential parameter ($S_{Ta_2} = 0.3187$), implying:*

- *Marketing efforts aimed at enhancing environmental awareness can yield significant returns in supply chain performance.*
- *Educational campaigns and green product promotion should be prioritized to leverage consumer sensitivity.*
- *The marginal effect of increasing a_2 is greater than that of operational parameters like α and c_0.*

Theorem 4.5 (Robustness and flexibility principle). *The varying sensitivity across parameters suggests:*

- ***Robustness focus**: High-sensitivity parameters (ρ, a_2) require tight control and monitoring.*
- ***Maintenance of flexibility**: Lower-sensitivity parameters (α, c_0) can be managed with greater flexibility.*
- ***Allocation of resources**: Management resources should be allocated proportionally to parameter sensitivity rankings.*

Corollary 4.3 (Design of the monitoring system). *Based on Theorems 4.3 and 4.5:*

- *Establish continuous monitoring systems for ρ and a_2 with early warning mechanisms.*

- *Implement real-time tracking of financial and market sensitivity parameters.*
- *Develop adaptive thresholds based on sensitivity rankings.*

Corollary 4.4 (Integration of the decision framework)**.** *From Theorems 4.3 and 4.4:*

- *Create integrated decision systems that simultaneously consider financial and market parameters.*
- *Develop cross-functional coordination mechanisms between finance and marketing departments.*
- *Implement feedback loops between financial incentives and market response.*

Corollary 4.5 (Resource allocation strategy)**.** *Following Theorem 4.5:*

- *Allocate monitoring resources proportionally to the Sobol sensitivity rankings, with higher priority given to ρ and a_2.*
- *Prioritize investment in financial management capabilities and consumer's sensitivity to the greenness of the product.*
- *Develop specialized teams for the management of high-sensitivity parameters.*

Theorem 4.6 (Global sensitivity management principle)**.** *For complex GSCS under uncertainty, management effectiveness is maximized when:*

- *The parameter monitoring priority follows the Sobol sensitivity rankings:*

$$\rho \to a_2 \to \theta \to \tau \to \alpha \to c_0.$$

- *In the context of interest rate reduction, strategic decisions must account for parameter interaction effects, even those that appear weak under baseline conditions, since changes in the financial environment can amplify their influence on system stability and performance.*
- *Resource allocation is proportional to parameter influence magnitudes.*
- *Adaptive strategies are implemented based on on the results of the sensitivity analysis.*

Proof. This theorem synthesizes the results from Theorems 4.2-4.5 and Lemma 4.1-4.2, establishing a comprehensive framework for managing complex supply chains based on global sensitivity analysis. The proof follows from the logical integration of the preceding theorems and their practical implications. □

Remark 4.3. The proposed theorem framework provides a mathematically rigorous foundation for managing green supply chains under uncertainty. By quantifying the influences of the parameters and the effects of the interaction, managers can make evidence-based decisions with predictable outcomes. The framework is particularly valuable for complex systems where multiple parameters interact in non-linear ways, as illustrated in Figure 1.

The theoretical framework established in this section provides a rigorous mathematical foundation for understanding and managing the complex dynamics of green supply chains. The results of the sensitivity analysis demonstrate that the financial parameters (ρ) and market factors (a_2) dominate the behavior of the system, requiring prioritized management attention. The interaction effects highlight the necessity of integrated decision-making approaches rather than isolated parameter optimization. Compared with the local sensitivity analysis in Subsection 4.1, the global Sobol analysis quantifies the overall influence of parameters and their weak interaction effects across the entire parameter space, providing a more comprehensive basis for managerial decisions.

Table 10. Summary of Sobol sensitivity ranking and management priorities.

Parameter	Symbol	Ranking	Management Priority
Discount rate	ρ	1	Primary focus
Consumer's green sensitivity	a_2	2	Strategic attention
Price weight coefficient	θ	3	Coordinated management
Time delay	τ	4	Monitoring required
Green investment cost	α	5	Flexible control
Unit production cost	c_0	6	Baseline monitoring

5. Numerical simulation

In this section, we support the above theoretical results by providing associate numerical examinations with the virtue of Matlab.

5.1. Sensitivity analysis

In this research, the discount rate ρ is important, because it affects the present value of the total profit. From Subsection 4.1, as ρ belongs to the real number field, we obtain the influence of the discount rate ρ on g_1^* for the centralized model and the impact of ρ on g_2^* in the decentralized model. Next, we support the results by numerical simulation. The numerical simulation about the effects of other parameters on g_1^* and g_2^* can be obtained by a similar method, and here we omitted them.

For the centralized model, we select a set of diverse parameter values (different from the baseline in Table 1) to demonstrate the robustness of our analytical results. Choosing $\delta = 0.9,\ a_1 = 0.8,\ a_2 = 0.5,\ a = 500,\ \alpha = 10,\ c_0 = 10,\ b = 0.6$, the expression of g_1^* about ρ is $g_1^* = 248/(3.6\rho + 2.74)$. From the Figure 2 (a), as $\rho < 0.761$, g_1^* goes down as ρ goes up but $g_1^* < 0$, so this case lacks of meaning; As $\rho > 0.761$, we can see that $g_1^* > 0$ is negative related with ρ, and the more detailed exhibition can obtained from Figure 2 (b).

For the decentralized model, keep the values of all parameters the same as in the centralized model. The expression of g_2^* about ρ is $g_2^* = 377/(5.76\rho + 4.434)$. From Figure 2 (c), as $\rho < 0.77$, g_2^* goes down as ρ goes up but $g_2^* < 0$, so this case lacks of meaning also; As $\rho > 0.77$, $g_2^* > 0$ is also negative related to ρ, and a more detailed exhibition can be obtained from Figure 2 (d).

This phenomenon explains that the increment of the discount rate of the product will cause the reduction of the greenness of the product.

Next, we will use the 3D Sobol index visualization program to plot 3D visual graphs of the global sensitivity analysis results, which are displayed in Figure 3.

For Figure 3, the Subfigure (a) displays the three-dimensional comparison of first-order and total-effect Sobol indices, showing the dominant influence of ρ and negligible parameter interactions; The Subfigure (b) is the parameter interaction matrix, where diagonal elements represent first-order indices and off-diagonal elements indicate weak interactions; The Subfigure (c) shows the radar chart analysis of multi-parameter influences, confirming the ranking $\rho \succ a_2 \succ \theta \succ \tau \succ \alpha \succ c_0$; The Subfigure (d) supports the cumulative contribution progression analysis, demonstrating that ρ and a_2 together explain approximately 80% of the output variance.

Next, we focus on the effects of the discount rate ρ and delay term τ on the stability of the positive equilibrium. Taking the centralized decision-making model as an example, when system

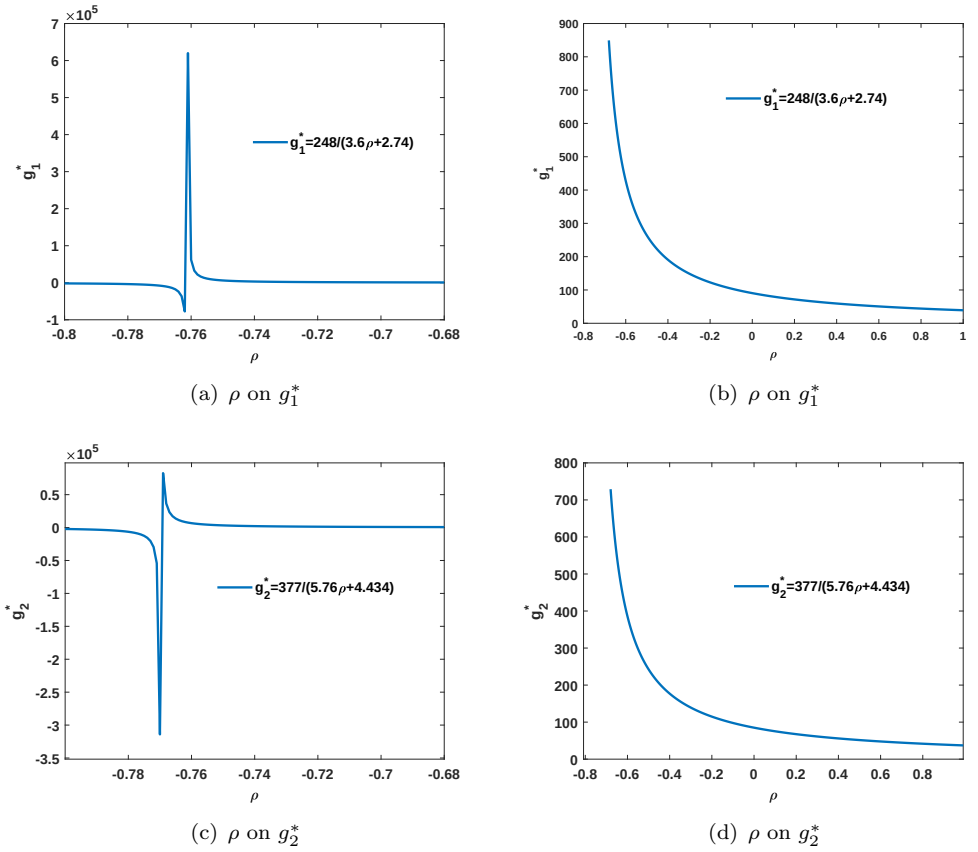

(a) ρ on g_1^* (b) ρ on g_1^*

(c) ρ on g_2^* (d) ρ on g_2^*

Figure 2. The influence of ρ on g_1^* and the impact of ρ on g_2^*.

(2.17) is without delay, we show mainly how ρ affects the existence and stability of the positive equilibrium through numerical simulation.

5.2. Existence and stability of the positive equilibrium

By Table 6 and Theorem 2.1, we can select the parameters group G_1 in Table 11, which satisfies $a_1 > b$. By the expressions of A_1 and A_2, we have $A_1 = 248 > 0$, $A_2 = 3.1 > 0$, $A_1A_2 > 0$. Clearly, the conditions of Theorem 2.2 are satisfied. So the unique positive equilibrium $E_1(72,\ 712.1429)$ exists and the other values are shown in V_1 of Table 12. $A_2 > 0$ satisfies condition (i) of Theorem 2.2, so E_1 is a saddle and its orbit is displayed in the Subfigure (a) of

Table 11. Parameter assignment table.

	a	a_2	α	δ	c_0	ρ	a_1	b	μ
G_1	500	0.5	10	0.9	10	0.1	0.8	0.6	0.6
G_2	5000	0.99	0.1	0.9	5001	0.02	0.8	0.3	0.5
G_3	5000	0.99	0.1	0.9	5001	−0.02	0.8	0.3	0.5
G_4	5000	0.99	0.1	0.9	5001	0	0.8	0.3	0.5

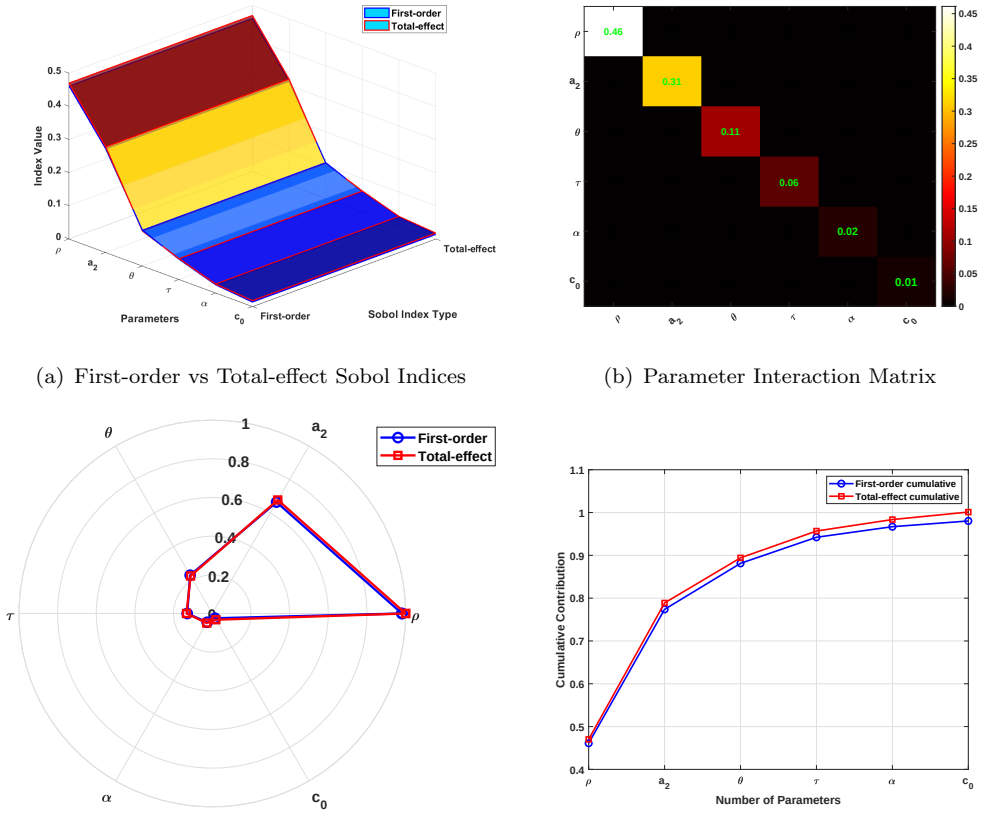

(a) First-order vs Total-effect Sobol Indices

(b) Parameter Interaction Matrix

(c) Radar Chart Comparison

(d) Cumulative Contribution Analysis

Figure 3. The 3D visual graphs of the global sensitivity analysis results.

Figure 4. Now, this situation has nothing to do with ρ. Next, we choose three parameter groups with different ρ, which is displayed in $G_2 - G_4$. In G_2, $\rho = 0.02 > 0$; In G_3, $\rho = -0.02 < 0$; In G_4, $\rho = 0$.

Table 12. The other values and the nature of E_1.

	g_1^*	p_{m1}^{0*}	D_{m1}^*	D_{r1}^*	**Nature of E_1**
V_1	80	747.8571	169	119	**Saddle**
V_2	0.5273	5001.0221	0.011	0.011	**Unstable focus**
V_3	0.5263	5001.0211	0.0105	0.0105	**Stable focus**
V_4	0.5268	5001.0216	0.0108	0.0108	**Center**

Choosing G_2 in Table 11, $A_1 = -0.99 < 0$, $A_2 = -1.8774 < 0$, $A_1A_2 > 0$, and $\rho > 0, A_2 < 0$, $2A_2 + \rho^2\alpha(a_1 - b) = -3.7548 < 0$ are satisfied. Clearly, the conditions of Theorem 2.1 and situation (ii) of Theorem 2.2 are satisfied. So $E_1(0.4746, 5001.0221)$ exists and it is an unstable focus. Its orbit phase is the Subfigure (b) of Figure 4. Other values are in V_2 of Table 12.

Taking G_3 of Table 11, then $A_1 = -0.99 < 0$, $A_2 = -1.881 < 0$, $A_1A_2 > 0$, so $\rho < 0, A_2 < 0$ and $2A_2 + \rho^2\alpha(a_1 - b) = -3.7620 < 0$ hold. Clearly, by Theorem 2.1 and the condition (iii) of

Theorem 2.2, $E_1(0.4737, 5001.0211)$ exists and it is a stable focus. Its phase is shown in Figure 4 (c). Others are displayed in V_3 of Table 12.

Choosing G_4 of Table 11, $A_1 = -0.99 < 0$, $A_2 = -1.8792 < 0$ and $A_1A_2 > 0$, these meet conditions $\rho = 0, A_2 < 0$. Clearly, by Theorem 2.1 and condition (iv) of Theorem 2.2. So $E_1(0.4741, 5001.0216)$ is a center. The other values are in V_4 of Table 12. Its phase is the Subfigure (d) of Figure 4.

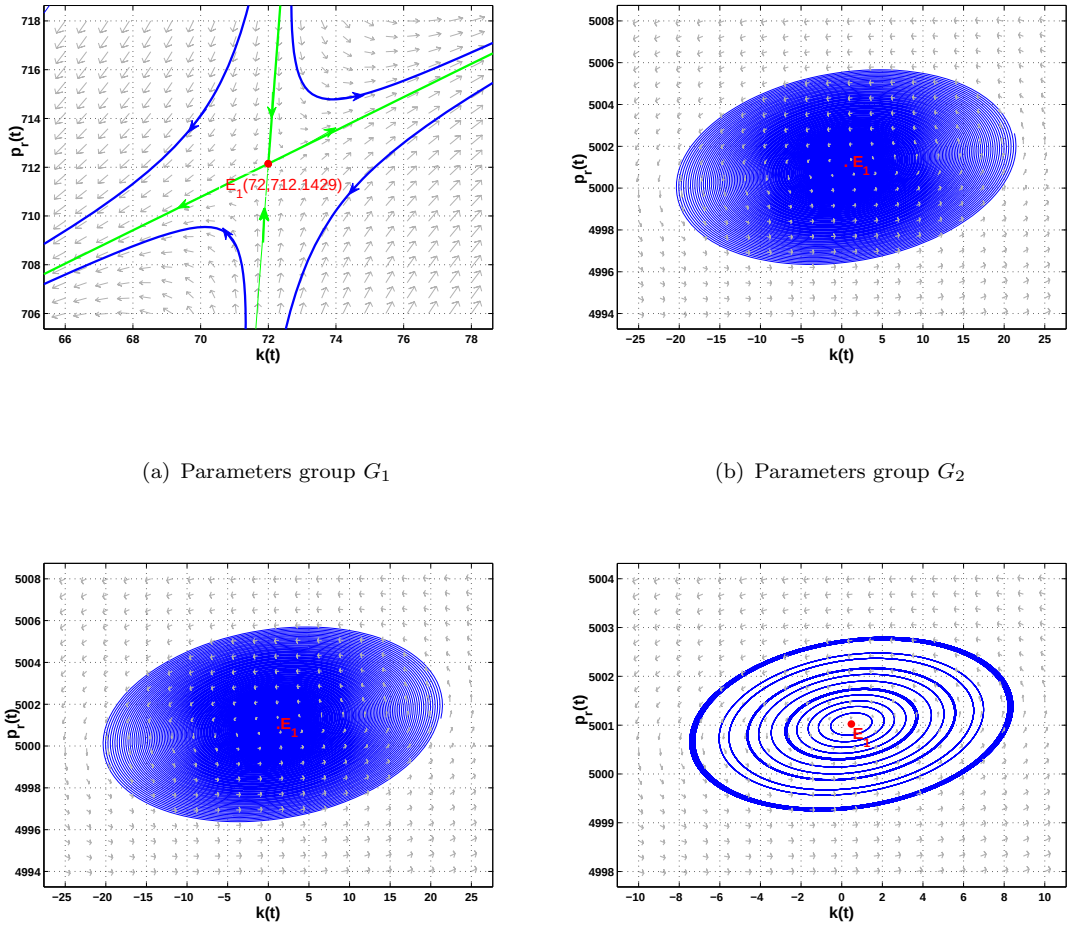

(a) Parameters group G_1

(b) Parameters group G_2

(c) Parameters group G_3

(d) Parameters group G_4

Figure 4. Local stability of the equilibrium E_1.

In Figure 4, these lines denote the solution curves $(k(t), p_m(t))$ of the system (2.18) near E_1. The arrows in the direction field represent the direction of the solution curves. From Figure 4 (a), one green line is convergent to E_1, and the other is far away from E_1, showing E_1 is unstable. By the direction of the blue lines, E_1 is a saddle. From Figure 4 (b), the solution curve is a spiral rotating away from the equilibrium E_1, or there is a spiral source at E_1, so E_1 is an unstable focus. In Figure 4 (c), the solution curve is a spiral that rotates around the equilibrium E_1, or there is a spiral sink at E_1, so E_1 is a stable focus. In Figure 4 (d), solution

curves are a series of periodic closed trajectories that are not isolated, so E_1 is a center and it seems like a Neutrally-stable center. The changes from Figure 4 (b) to Figure 4 (d) and then from Figure 4 (d) to Figure 4 (c) supports the theoretical result that equilibrium E_1 changes from the unstable focus to the center and then from the center to the stable focus as ρ from positive to zero and then from zero to negative.

The existence and local stability of positive equilibrium in decentralized model can be obtained by the same way, here we omitted it.

Next, we show the effect of the delay term τ on the stability of the positive equilibrium. Still, taking the centralized decision-making model as the example, when the positive equilibrium E_1 is stable, we display how τ affects the stability of equilibrium E_1.

5.3. Hopf bifurcation

Subsection 2.2.3 establishes the Hopf bifurcation criteria for system (2.17) with respect to the delay parameter τ and the weight coefficient θ. First, we consider the characteristic equation of the linearized neutral delay system (2.19):

$$(\gamma^2 - \rho\gamma + S_1)\big[\theta + (1-\theta)e^{-\gamma\tau}\big] = 0,$$

where S_1 is a constant derived from the model parameters. For the system to undergo a Hopf bifurcation, purely imaginary roots $\gamma = i\omega$ $(\omega > 0)$ must appear in the characteristic equation.

Setting $\gamma = i\omega$ and analyzing the critical case, we find that purely imaginary roots emerge when $\theta = 0.5$. This result is formally stated in Theorem 2.3: If $0 < \theta < 0.5$, the equilibrium $E_1(k_1^*, p_{m1}^{0*})$ is unstable for all $\tau > 0$; if $\theta > 0.5$, E_1 is stable for all $\tau > 0$. The transition point $\theta = 0.5$ indicates the occurrence of a Hopf bifurcation, as non-hyperbolic equilibrium and purely imaginary roots appear. To further confirm this analytical result, we conduct numerical simulations.

Fix the other parameter group as G_3 of Table 11, and the positive equilibrium E_1 is stable focus as the system (2.17) is without delay term (see the phase (c) in Figure 4). Next, fixed $\tau = 5$, choosing θ differently, we can obtain the following figures.

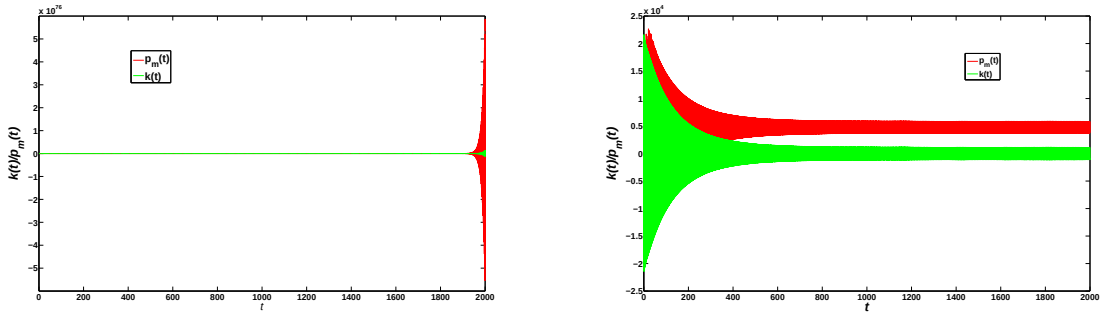

(a) θ=0.4 (b) θ=0.6

Figure 5. Change of stability for E_1 as θ increases.

In Figure 5, the green lines denote $k(t)$ and the red lines stand for $p_r(t)$. As shown in Figure 5, with τ fixed, the equilibrium E_1 is unstable when $\theta = 0.4 < 0.5$ (see the red line from Figure 5 (a)). We can see that E_1 becomes stable when $\theta = 0.6 > 0.5$ (see the green line from Figure

5 (b)). This numerical evidence clearly illustrates the stability switching at $\theta = 0.5$, which is consistent with our analytical bifurcation criteria.

Remark 5.1. From the above analysis, we can see how τ and θ plays a role in system (2.17). Under the parameter group G_3 in Table 11, if $\theta = 1,\ \tau = 0$, then E_1 is a stable focus, as shown in phase (c) in Figure 4. If $\theta\tau \neq 0$, $\tau > 0$, then the stability of E_1 changes with θ increasing. E_1 is unstable as $0 < \theta < 0.5$, and E_1 is stable when $0.5 < \theta < 1$, and Figure 5 supports Hopf bifurcation occurs for θ=0.5.

The existence of Hopf bifurcation in the decentralized model can be derived similarly, and we omit the repetitive derivation for brevity.

This Hopf bifurcation analysis further confirms that θ acts as a critical stability switch, which is consistent with the sensitivity-stability correlation in next subsection.

5.4. Correlation between sensitivity indices and stability regions

In this subsection, we further investigate the relationship between parameter sensitivity and system stability by visualizing the stability regions. Combined with the Sobol global sensitivity indices, Table 13 establishes a direct correlation between the total-effect indices and the stability contributions of key parameters, and two additional figures are presented to intuitively demonstrate how the top-ranked sensitive parameters dominate the system stability boundaries.

Table 13. Correlation between parameter sensitivity indices and system stability contributions.

Parameter	Ranking	Contribution to System Stability	Critical Stability Threshold
ρ	1	Dominates system stability type; determines stable/unstable/center states	$\rho < 0$ (stable); $\rho > 0$ (unstable)
a_2	2	Determines the sign of A_2/B_2; dominates equilibrium existence and stability	$a_2^2 < \alpha\delta(\rho+\delta)(a_1-b)$ (stable focus)
θ	3	Acts as a stability switch; induces Hopf bifurcation	$\theta > 0.5$ (stable for all $\tau > 0$); $\theta < 0.5$ (unstable)
τ	4	Amplifies instability but does not change stability	No critical stability threshold
α	5	Indirectly influences stability by affecting A_2/B_2	$\alpha > \dfrac{a_2^2}{\delta(\rho+\delta)(a_1-b)}$ (saddle)
c_0	6	Only affects equilibrium location; no impact on stability	No critical stability threshold

As summarized in Table 13, the parameters with the highest Sobol total-effect indices (i.e., ρ, a_2, and θ) are precisely the critical factors that govern the stability of the system equilibrium. Specifically, the discount rate ρ (ranked 1st) directly determines the stability type (stable/unstable/center) through its sign change, while the consumer green sensitivity a_2 (ranked 2nd) and price weight coefficient θ (ranked 3rd) control the existence of stable equilibria and induce stability switching (e.g., Hopf bifurcation at $\theta = 0.5$). In contrast, low-sensitivity parameters (e.g., τ, α, c_0) exert no direct influence on the stability type, only modifying the equilibrium position or amplifying existing instability. Figure 6 visualizes the stability distribution in the

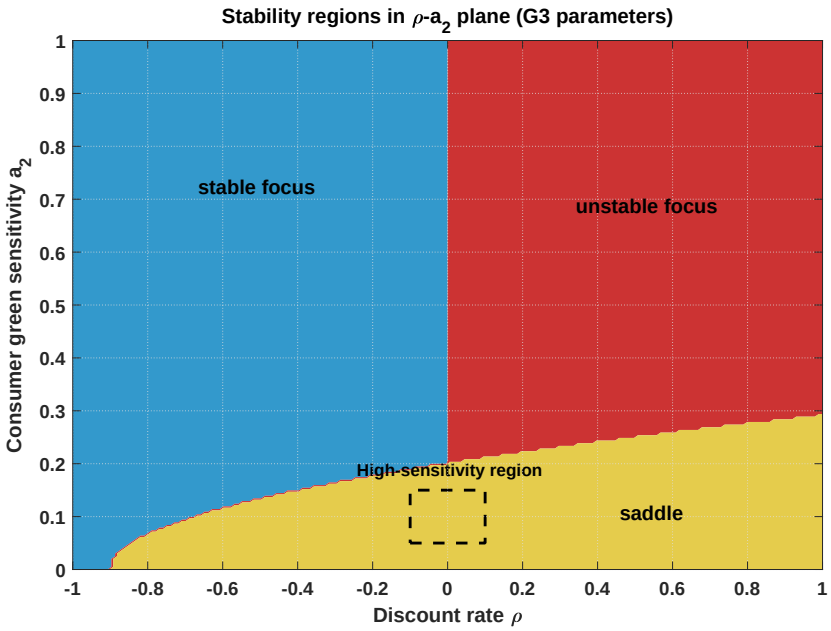

Figure 6. Stability regions in the ρ-a_2 plane with fixed $\theta = 0.6$ and $\tau = 5$, Taking other parameters from G_3 of Table 11.

ρ-a_2 parameter plane. To clearly demonstrate the stability transition and facilitate a direct comparison with the stable focus case V_3, we appropriately expand the coordinate ranges of ρ and a_2. The high-sensitivity region is exactly located at the boundary between the stable and unstable regions, confirming that the most influential parameters govern the system stability. The blue area represents the stable focus state (corresponding to case V_3 in Table 11), the red area represents the unstable focus state (corresponding to case V_2), and the yellow area represents the saddle-point state (corresponding to the similar case V_1). The dashed rectangle marks the high-sensitivity interval of ρ and a_2, which lies exactly at the boundary between the stable and unstable regions, confirming that the top-ranked sensitive parameters govern the system stability transitions.

From Figure 7, we can see the oscillation amplitude versus θ for different time delays τ, with other parameters taken from group G_3 in Table 10. The dashed vertical line denotes the Hopf bifurcation at $\theta = 0.5$, separating the unstable region ($\theta < 0.5$) and stable region ($\theta > 0.5$). Larger time delays τ amplify the oscillation amplitude in the unstable region, while all curves decay to zero in the stable region. An interesting and important observation emerges from the stable region: When $\tau = 0$ and $\theta = 1$, the oscillation amplitude is exactly zero, signifying that the system is fully stable and converges to the equilibrium without any oscillations. This result perfectly aligns with the stable focus equilibrium V_3 presented in Table 13, providing direct numerical evidence that the system achieves asymptotic stability under appropriate parameter settings. This consistency between the numerical simulation and the theoretical classification of equilibrium types further validates the robustness of our stability analysis.

This integrated analysis of the correlation table and stability visualizations explicitly links the Sobol sensitivity indices to the system stability regions, significantly enhancing the interpretability of the results and providing a rigorous theoretical foundation for targeted management strategies in green supply chain dynamics.

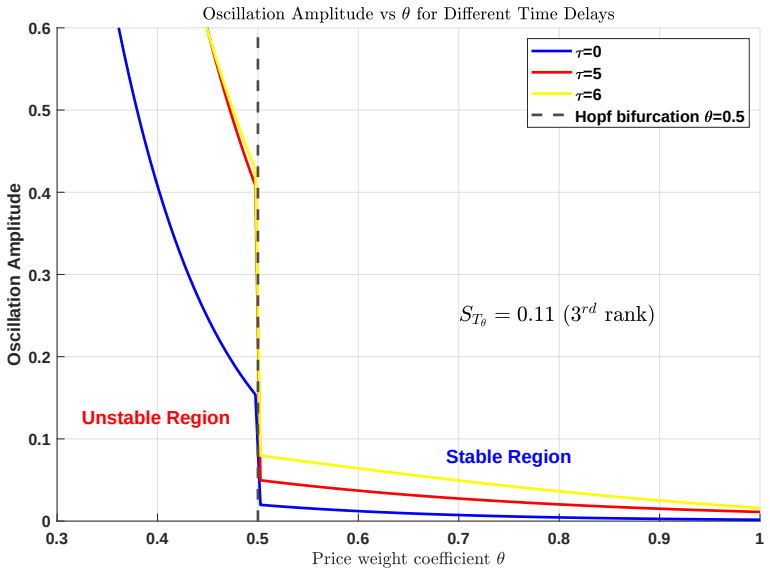

Figure 7. Oscillation amplitude versus θ for different time delays τ (Taking other parameters from G_3).

6. Conclusions and managerial implications

It is an established fact that the positive discount rate plays an essential role in constructing the objective function. However, the impact of the negative discount rate is still unclear. Here, based on the extension of discount rate to the whole real number domain, we investigate a two-channel green supply chain neutral delay differential system with respect to the green technology level and the price of the manufacturer under centralized and decentralized decision making, respectively. For two neutral delay differential systems, we consider the existence of the positive equilibria. Under the condition of making sure that the positive equilibria exist, the local stability are investigated. Compared to the result about the stability of the equilibria in the single channel work [23], in this research, due to the widening range of discount rates, the equilibrium of both the centralized and decentralized models may be stable, rather than always being a saddle. Moreover, under the equilibrium remains stable as $\tau = 0$, taking θ as the bifurcation parameter, Hopf bifurcation occurs for θ=0.5. Stability analysis reveals that the introduction of delay can induce Hopf bifurcation, creating periodic fluctuations that managers must account for in strategic planning.

Furthermore, by comparing the equilibria obtained in two decision-making scenarios, we know that, although the optimal profit in the centralized decision-making system outperforms the total profit of the decentralized system (as shown in Table 2), it is often difficult to implement in practice due to the challenges of unified strategy-making among independent members. Therefore, designing an effective coordination mechanism to achieve Pareto improvements for all members is essential. So we design a cooperation and coordination model by introducing the transfer payment mechanism to make the GSCs members achieve a win-win. Thus, we recommend the upstream and downstream companies of dual channel GSCs to adopt the cooperation and coordination model if they can not accept the centralized GSCs. Because the proposed wholesale-price-based transfer payment mechanism effectively coordinates decentralized systems, enabling Pareto improvements for both manufacturers and retailers.

Next, we have established that the extended discount rate $\rho \in \mathbb{R}$ (including negative values) and the consumer's green sensitivity a_2 emerge as the most influential parameters in green supply chain dynamics. These findings offer several actionable insights for supply chain practitioners in Subsection 4.2.

Although this research provides substantial insights, several limitations suggest directions for future investigation. First, our model assumes identical delay parameters for manufacturers and retailers; future work could explore asymmetric delay scenarios. Second, the study focuses on a two-echelon supply chain; extending this to multi-echelon networks would enhance practical applicability. Third, we considered deterministic parameters; incorporating stochastic elements would better reflect real-world uncertainties. Finally, empirical validation of the proposed coordination mechanism across different industry contexts would strengthen the practical contributions. Despite these limitations, this research provides a robust theoretical foundation for understanding and managing dual channel green supply chains with time delay effects. Integration of differential game theory, bifurcation analysis, and global sensitivity analysis offers a comprehensive approach to addressing complex supply chain dynamics in environmentally conscious market environments.

Conflict of interest

The authors declare that they have no conflict of interest.

References

[1] S. İ. Araz, *Analysis of a covid-19 model: Optimal control, stability and simulations*, Alex. Eng. J., 2021, 60(1), 647–658.

[2] İ. A. Arık and S. İ. Araz, *Delay differential equations with fractional differential operators: Existence, uniqueness and applications to chaos*, Commun. Anal. Mech., 2024, 16(1), 169–192.

[3] C. Arteta, A. Kose, M. Stocker and T. Taskin, *Negative Interest Rate Policies: Sources and Implications (English)*, Policy Research Working Paper No. WPS7791, Washington, D.C., World Bank Group, 2016.

[4] L. Bo, M. Zhu, Y. Jiang and Z. Li, *Pricing policies of a competitive dual-channel green supply chain*, J. Clean. Prod., 2016, 112(3), 2029–2042.

[5] S. Cecchetti, *The case of the negative nominal interest rates: New estimates of the term structure of interest rates during the great depression*, J. Polit. Econ., 1988, 96(6), 1111–1141.

[6] J. Chen, H. Zhang and Y. Sun, *Implementing coordination contracts in a manufacturer stackelberg dual-channel supply chain*, Omega, 2012, 40(5), 571–583.

[7] J. Dai, D. Cantor and F. Montabon, *How environmental management competitive pressure affects a focal firm's environmental innovation activities: A green supply chain perspective*, J. Bus. Logist., 2015, 36(3), 242–259.

[8] Y. Dou, Q. Zhu and J. Sarkis, *Green multi-tier supply chain management: An enabler investigation*, J. Purch. Supply Manag., 2018, 24(2), 95–107.

[9] Y. Du and C. Zhang, *The effects of delays on stability and spatiotemporal dynamics in a diffusive nutrient-phytoplankton model*, Chaos Solitons Fractals, 2025, 199, 116809.

[10] C. Ghisetti and F. Quatraro, *Green technologies and environmental productivity: A cross-sectoral analysis of direct and indirect effects in italian regions*, Ecol. Econ., 2017, 132, 1–13.

[11] M. Guo, J. Nowakowska-Grunt, V. Gorbanyov and M. Egorova, *Green technology and sustainable development: Assessment and green growth frameworks*, Sustainability, 2020, 12(16), 6571.

[12] Z. Guo, J. Liu, B. Li and T. Zhang, *Stability analysis of a delayed predator-prey model with generalist predator and fear effect*, Chaos Solitons Fractals, 2026, 202, 117448.

[13] M. Johari, S.-M. Hosseini-Motlagh and M. Rasti-Barzoki, *An evolutionary game theoretic model for analyzing pricing strategy and socially concerned behavior of manufacturers*, Transport. Res. E.-Log., 2019, 128, 506–525.

[14] Y. kuang, *Delay Differential Equations: With Applications in Population Dynamics*, Academic Press, Boston, 1993.

[15] C.-L. Li, *Quantifying supply chain ineffectiveness under uncoordinated pricing decisions*, Oper. Res. Lett., 2008, 36(1), 83–88.

[16] S. Li, S. Yuan, Z. Jin and H. Wang, *Bifurcation analysis in a diffusive predator-prey model with spatial memory of prey, Allee effect and maturation delay of predator*, J. Differ. Equ., 2023, 357, 32–63.

[17] T. Li and J. Ma, *Complexity analysis of the dual-channel supply chain model with delay decision*, Nonlinear Dyn., 2014, 78(1), 2617–2626.

[18] L. Liu, *Research on the management system of enterprises using modern logistics supply chain theory*, Procedia Eng., 2021, 24, 721–725.

[19] P. Liu and Z. Ali, *Hamacher interaction aggregation operators for complex intuitionistic fuzzy sets and their applications in green supply chain management*, Complex Intell. Syst., 2024, 10(3), 3853–3871.

[20] Y. Lv, *The spatially homogeneous Hopf bifurcation induced jointly by memory and general delays in a diffusive system*, Chaos Solitons Fractals, 2022, 156, 111826.

[21] Y. Lv, *Global boundedness and spatially inhomogeneous hopf bifurcation in a delayed predatorščprey model with dual taxis*, Chaos Solitons Fractals, 2025, 201, 117369.

[22] M. D. McKay, R. J. Beckman and W. J. Conover, *A comparison of three methods for selecting values of input variables in the analysis of output from a computer code*, Technometrics, 1979, 21(2), 239–245.

[23] A. Mohsin, S. Far Abid Hossain, H. Tushar, et al., *Differential game model and coordination model for green supply chain based on green technology research and development*, Heilyon, 2021, 7(8), e07811.

[24] A. Mohsin, H. Lei and S. Far Abid Hossain, *Impact of covid-19 pandemic on consumer economy: Countermeasures analysis*, SAGE Open, 2021, 11(2), 1–10.

[25] A. Mohsin, H. Lei, S. Far Abid Hossain, et al., *Operation and coordination mechanism of closed-loop supply chain considering corporate social responsibility behavior consciousness*, Cogent Bus. Manag., 2020, 7(1), 1845937.

[26] Q. Qi, J. Wang and Q. Bai, *Pricing decision of a two-echelon supply chain with one supplier and two retailers under a carbon cap regulation*, J. Clean. Prod., 2017, 151, 286–302.

[27] K. Rahmani and M. Yavari, *Pricing policies for a dual-channel green supply chain under demand disruptions*, Comput. Ind. Eng., 2019, 127, 493–510.

[28] L. Redding, *Negative nominal interest rates and the liquidity premium*, Econ. Lett., 1999, 62(2), 213–216.

[29] K. N. Salam, D. P. Ar and M. Rifai, *Member card and social media promotion strategies on customer loyalty*, J. Manaj. Bisnis, 2026, 13(1), 402–417.

[30] A. Saltelli, P. Annoni, I. Azzini, et al., *Variance based sensitivity analysis of model output. design and estimator for the total sensitivity index*, Comput. Phys. Commun., 2010, 181(2), 259–270.

[31] F. Si, J. Wang and X. Zou, *Stability analysis of price game model with delay in dual-channel supply chain*, J. Wuhan Univ. Technol., 2018, 40(4), 413–418.

[32] I. M. Sobol, *Global sensitivity indices for nonlinear mathematical models and their monte carlo estimates*, Math. Comput. Simul., 2001, 55(1–3), 271–280.

[33] H. Song and X. Gao, *Green supply chain game model and analysis under revenue-sharing contract*, J. Clean. Prod., 2018, 170, 183–192.

[34] J. Song, Y. He and Y. Duan, *Loss leader strategy in the live streaming considering cross-product and cross-channel spillover effects*, Int. J. Prod. Econ., 2026, 294, 109512.

[35] Q. Song and F. Yi, *Spatiotemporal patterns and bifurcations of a delayed diffusive predator-prey system with fear effects*, J. Differ. Equ., 2024, 388, 151–187.

[36] M. Subaşi and S. İ. Araz, *Numerical regularization of optimal control for the coefficient function in a wave equation*, Iran. J. Sci. Technol. Trans. Sci., 2019, 43(1), 2325–2333.

[37] E. Tirkolaee, A. Goli, M. Bakhsi and I. Mahdavi, *A robust multi-trip vehicle routing problem of perishable products with intermediate depots and time windows*, Numer. Algebra Control Optim., 2017, 7(4), 417–433.

[38] J. G. Vargas-Hernández, *Strategic transformational transition of green economy, green growth and sustainable development: An institutional approach*, Int. J. Environ. Sustain. Green Technol., 2020, 11(1), 34–56.

[39] A. Wan and X. Zou, *Hopf bifurcation analysis for a model of genetic regulatory system with delay*, J. Math. Anal. Appl., 2009, 356(2), 464–476.

[40] N. Wang, L. Qi, M. Bessane and M. Hao, *Global hopf bifurcation of a two-delay epidemic model with media coverage and asymptomatic infection*, J. Differ. Equ., 2023, 369, 1–40.

[41] W. Wang, L. Fan, P. Ma, et al., *Reward-penalty mechanism in a closed-loop supply chain with sequential manufacturers' price competition*, J. Clean. Prod., 2017, 168(1), 118–130.

[42] L. Xu, K. Mathiyazhagan, K. Govindan, et al., *Multiple comparative studies of green supply chain management: Pressures analysis*, Resour. Conserv. Recycl., 2013, 78(1), 26–35.

[43] X. Yu, Y. Lan and R. Zhao, *Strategic green technology innovation in a two-stage alliance: Vertical collaboration or co-development?*, Omega, 2021, 98, 102116.

[44] J. Zeng and B. Li, *Research on cooperation strategy between government and green supply chain based on differential game*, Open Math., 2019, 17(1), 828–855.

[45] J. Zhao and N. Sun, *Government subsidies-based profits distribution pattern analysis in closed-loop supply chain using game theory*, Neural. Comput. Appl., 2020, 32, 1715–1724.

[46] G. Zhou and C. Ju, *Effect analysis of service supply chain with dynamic game under the condition of sensitive demand*, Math. Probl. Eng., 2015, 2015, 278094.

[47] Y. Zhou and X. Ye, *Differential game model of joint emission reduction strategies and contract design in a dual-channel supply chain*, J. Clean. Prod., 2018, 190(20), 592–607.

[48] Q. Zhu, J. Sarkis and K.-H. Lai, *Institutional-based antecedents and performance outcomes of internal and external green supply chain management practices*, J. Purch. Supply Manag., 2013, 19(2), 106–117.

[49] Y. Zu, L. Chen and Y. Fan, *Research on low-carbon strategies in supply chain with environmental regulations based on differential game*, J. Clean. Prod., 2018, 177(10), 527–546.

[50] R. M. Zulqarnain, W. X. Ma, I. Siddique, H. Ahmad and S. Askar, *An intelligent MCGDM model in green suppliers selection using interactional aggregation operators for interval-valued pythagorean fuzzy soft sets*, Comput. Model. Eng. Sci., 2024, 139(2), 1829–1862.

Received October 2025; Accepted April 2026; Available online May 2026.